Vertical propagation of non–hydrostatic gravity waves into the mesosphere

Andreas Dörnbrack

DLR Oberpfaffenhofen

Institut für Physik der Atmosphäre

- Goals
- Methods
- Selected Cases
  - o Auckland RF23
  - o RF05

6^{th} EULAG-Workshop Warszaw 29 May 2018

Goals

- quasi-realistic numerical simulations of the flow across NZ and Auckland Islands from the surface to the mesosphere @ about 100 km
- understanding of the vertical propagation under
  - o different forcing conditions in the troposphere
  - o different stratospheric conditions for propagation
- compare with linear dynamics by conducting quasi-linear simulations
- try to reproduce the observed ‚broad spectra‘ and to understand the processes causing them

Methods

- 2D (later 3D) numerical simulations with EULAG (multiscale geophysical flow solver) integrating different approximations of the Navier-Stokes equations:
  - o compressible , pseudo-incompressible, anelastic, linearized versions
  - o inviscid
  - o lateral wave absorber
  - o vertical: exponentially increasing Rayleigh friction
- realistic topography along the mountain transects Mt Aspiring and Mt. Cook (taken from GV-data set)
- initial wind, potential temperature, density profiles:
  - o ECMWF IFS up to 80 km altitude
  - o NAVGEM* up to 100 km altitude

* Eckermann, S., D., J.Ma, K. W Hoppel, D. D Kuhl, D. R Allen, J. A. Doyle, K. C Viner, B. C Ruston, N. L Baker, S. D. Swadley, T. R. Whitcomb, C. A Reynolds, L. Xu, N. Kaifler, B. Kaifler, I. M Reid, D. J Murphy and P. T Love , 2018: High-Altitude (0-100 km) Global Data Assimilation System: Description and Application to the 2014 Austral Winter of the Deep Propagating Gravity-Wave Experiment (DEEPWAVE). *Mon. Wea. Rev.*, accepted.

Auckland Case RF23 14 July 2014

Dynamics of Orographic Gravity Waves Observed in the Mesosphere over the Auckland Islands during the Deep Propagating Gravity Wave Experiment (DEEPWAVE)

STEPHEN D. ECKERMANN,[a] DAVE BROUTMAN,[b] JUN MA,[b] JAMES D. DOYLE,[c] PIERRE-DOMINIQUE PAUTET,[d] MICHAEL J. TAYLOR,[d] KATRINA BOSSERT,[e] BIFFORD P. WILLIAMS,[e] DAVID C. FRITTS,[e] AND RONALD B. SMITH[f]

[a] *Space Science Division, U.S. Naval Research Laboratory, Washington, D.C.*
[b] *Computational Physics, Inc., Springfield, Virginia*
[c] *Marine Meteorology Division, U.S. Naval Research Laboratory, Monterey, California*
[d] *Center for Atmospheric and Space Sciences, Utah State University, Logan, Utah*
[e] *GATS, Inc., Boulder, Colorado*
[f] *Department of Geology and Geophysics, Yale University, New Haven, Connecticut*

Eckermann, S., D. Broutman, J. Ma, J. Doyle, P. Pautet, M. Taylor, K. Bossert, B. Williams, D. Fritts, and R. Smith, 2016: Dynamics of Orographic Gravity Waves Observed in the Mesosphere over the Auckland Islands during the Deep Propagating Gravity Wave Experiment (DEEPWAVE). *J. Atmos. Sci.,* 73, 3855–3876, doi: 10.1175/JAS-D-16-0059.1.

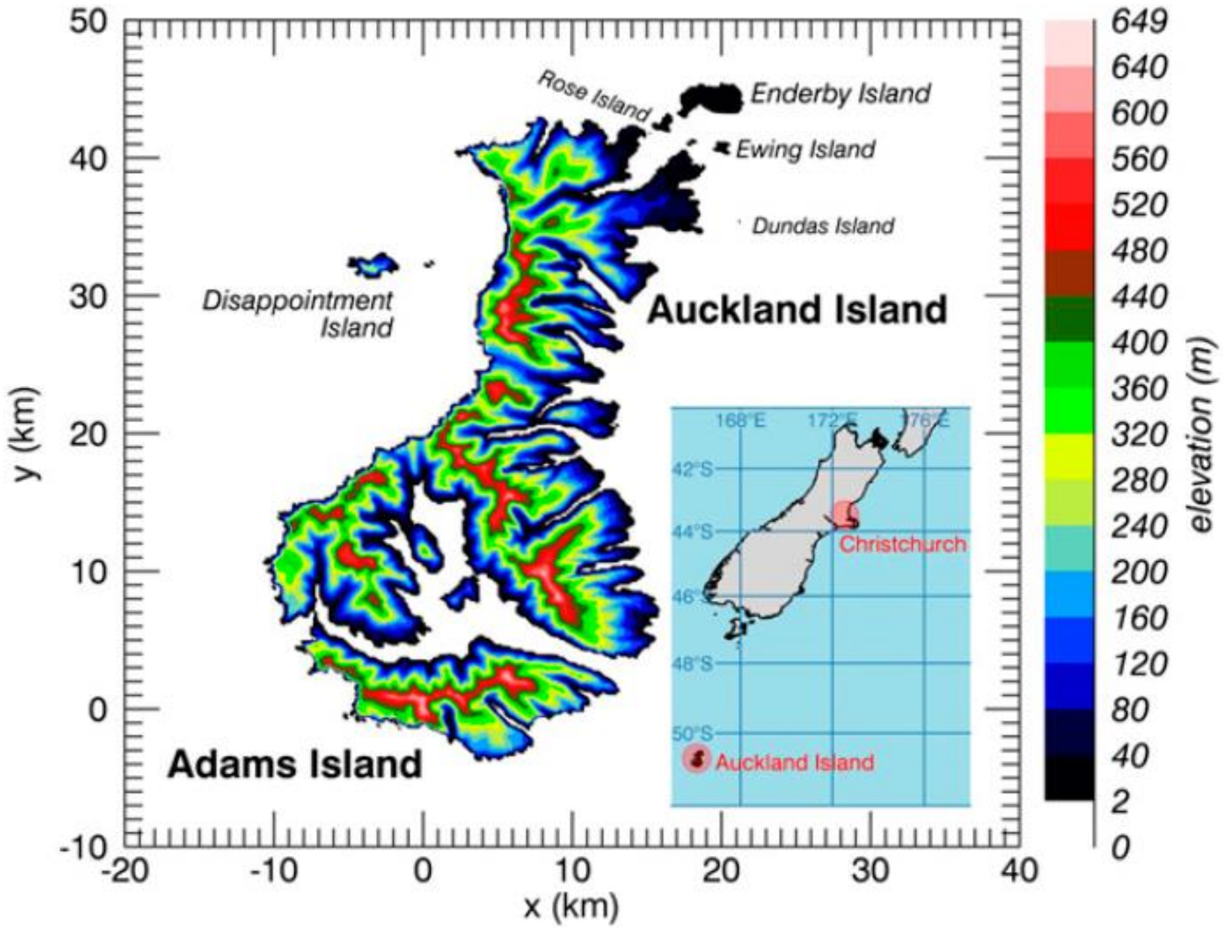

FIG. 1. Terrain elevations $h(x, y)$ of the Auckland Island archipelago derived from ASTER observations (see section 2c). Origin of (x, y) coordinate axes is located at Mount Dick, the highest peak. (inset) Map showing location of Auckland Island relative to DEEPWAVE operating base in Christchurch, New Zealand.

Eckermann, S., D. Broutman, J. Ma, J. Doyle, P. Pautet, M. Taylor, K. Bossert, B. Williams, D. Fritts, and R. Smith, 2016: Dynamics of Orographic Gravity Waves Observed in the Mesosphere over the Auckland Islands during the Deep Propagating Gravity Wave Experiment (DEEPWAVE). *J. Atmos. Sci.,* 73, 3855–3876, doi: 10.1175/JAS-D-16-0059.1.

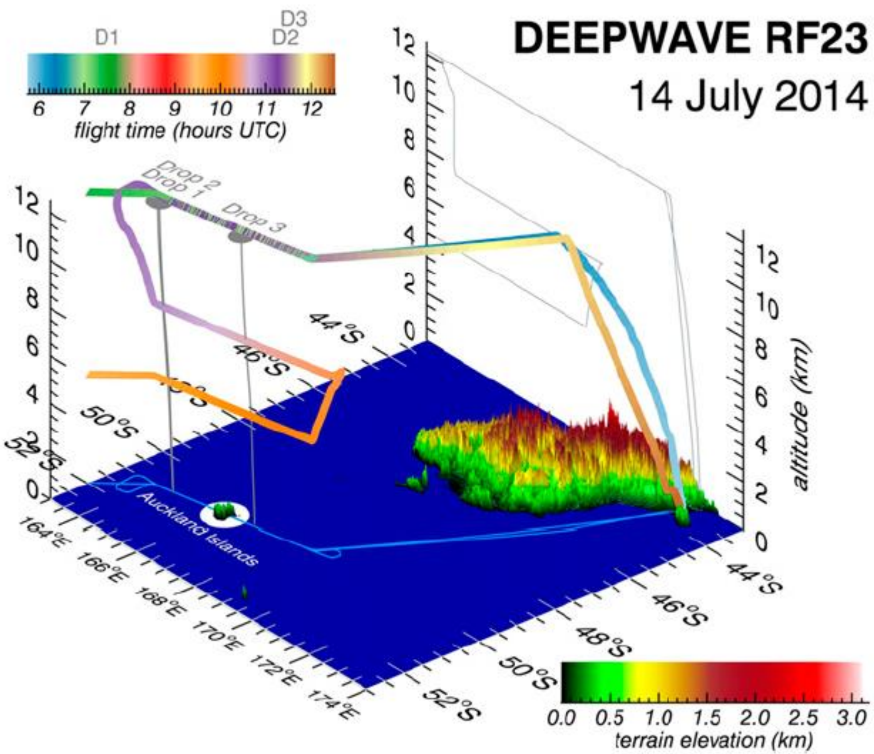

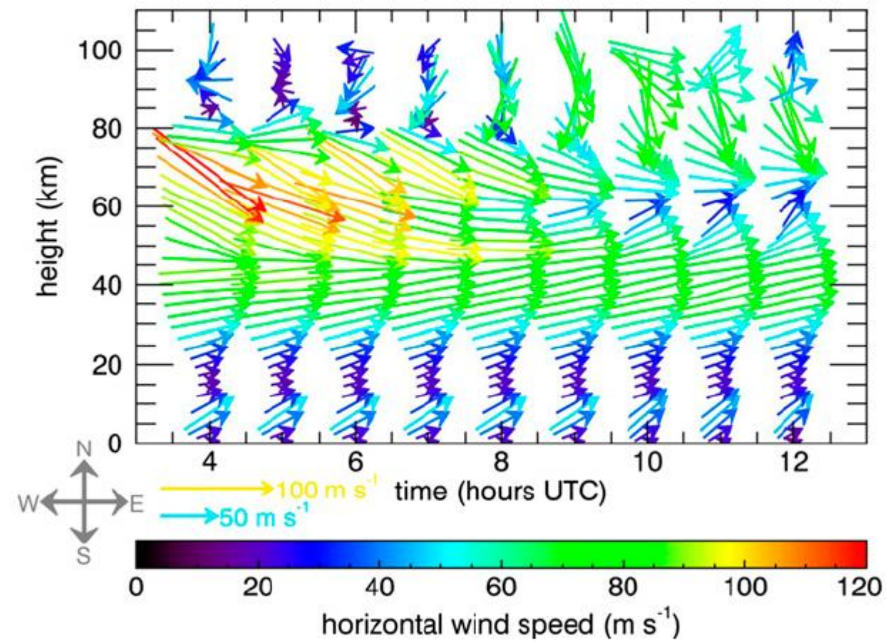

FIG. 4. Horizontal wind vectors upstream of Auckland Island on 14 Jul 2014 from NAVGEM reanalysis, plotted at hourly intervals from 0400 to 1200 UTC over the range z = 0–100 km.

Eckermann, S., D. Broutman, J. Ma, J. Doyle, P. Pautet, M. Taylor, K. Bossert, B. Williams, D. Fritts, and R. Smith, 2016: Dynamics of Orographic Gravity Waves Observed in the Mesosphere over the Auckland Islands during the Deep Propagating Gravity Wave Experiment (DEEPWAVE). *J. Atmos. Sci.,* 73, 3855–3876, doi: 10.1175/JAS-D-16-0059.1.

Observations at ~ 80 km altitude
14 July 2014

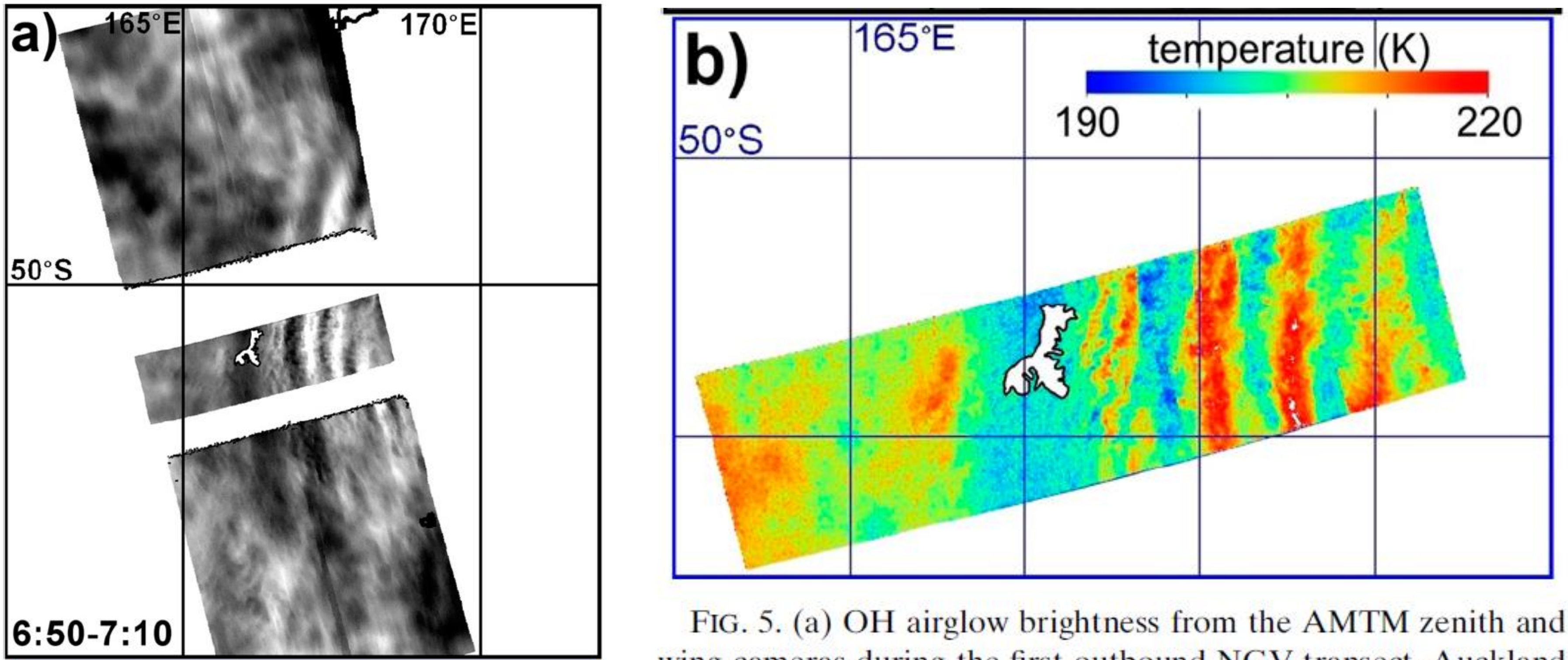

FIG. 5. (a) OH airglow brightness from the AMTM zenith and wing cameras during the first outbound NGV transect. Auckland Island is shaded white with the coastline outlined in black. Time span of these observations (UTC) is indicated at bottom left of this panel. (b) Rotational temperatures retrieved from the zenith camera airglow brightness in (a). See text and Pautet et al. (2016) for further details.

Eckermann, S., D. Broutman, J. Ma, J. Doyle, P. Pautet, M. Taylor, K. Bossert, B. Williams, D. Fritts, and R. Smith, 2016: Dynamics of Orographic Gravity Waves Observed in the Mesosphere over the Auckland Islands during the Deep Propagating Gravity Wave Experiment (DEEPWAVE). *J. Atmos. Sci.*, 73, 3855–3876, doi: 10.1175/JAS-D-16-0059.1.

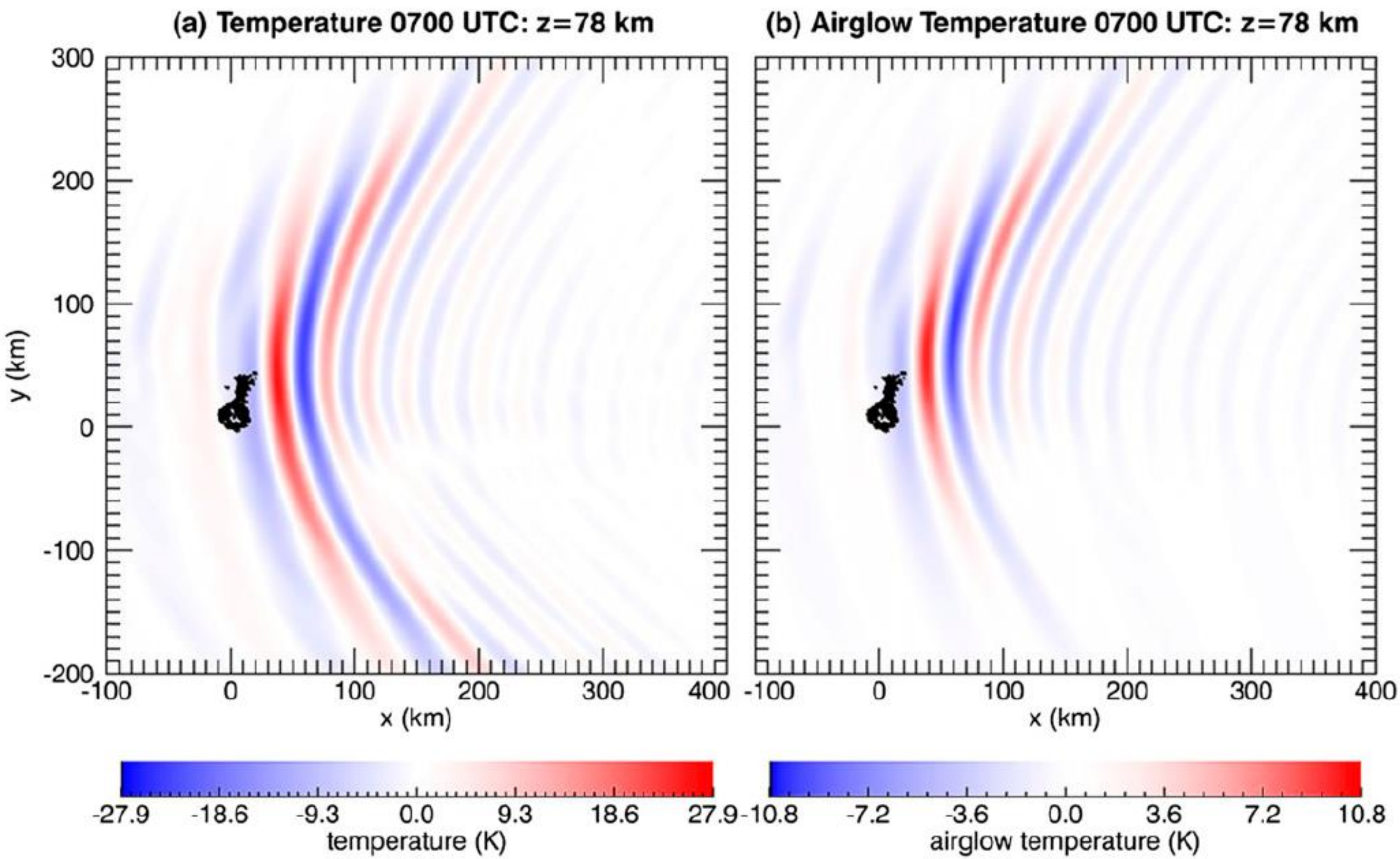

FIG. 11. (a) $T'(x, y, z, t_c)$ Fourier solution (K; color bar) at $z = 78$ km and $t_c = 4$ h, calculated using NAVGEM background profiles at 0700 UTC. (b) Modified solutions after applying the airglow filter function $S_{\mathrm{AG}}(m)$ in (17) via (3).

Eckermann, S., D. Broutman, J. Ma, J. Doyle, P. Pautet, M. Taylor, K. Bossert, B. Williams, D. Fritts, and R. Smith, 2016: Dynamics of Orographic Gravity Waves Observed in the Mesosphere over the Auckland Islands during the Deep Propagating Gravity Wave Experiment (DEEPWAVE). *J. Atmos. Sci.,* 73, 3855–3876, doi: 10.1175/JAS-D-16-0059.1.

Vertical Profiles 14 July 2014 06 UTC

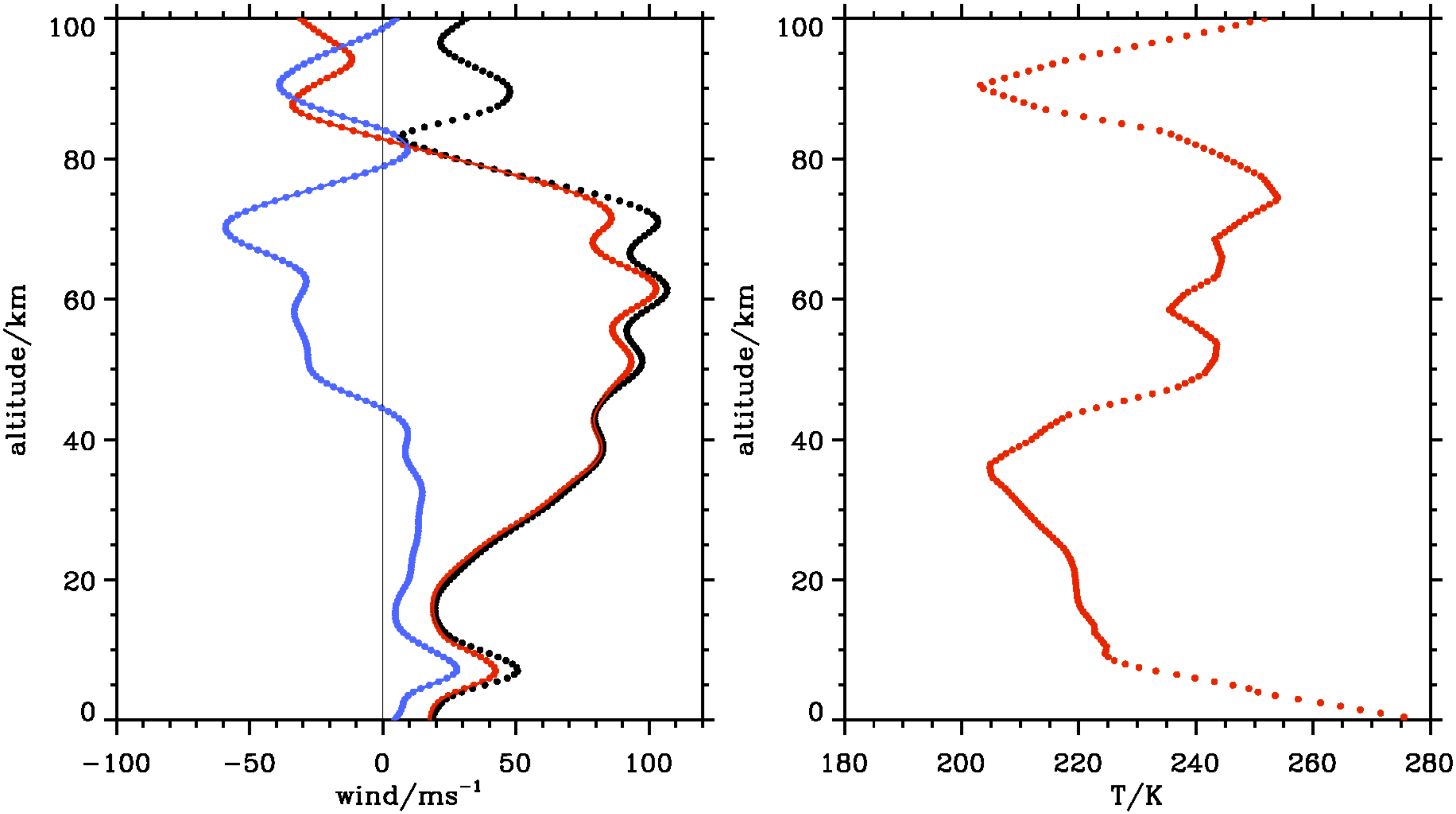

meridional component
zonal component
horizontal wind

t = 0 min

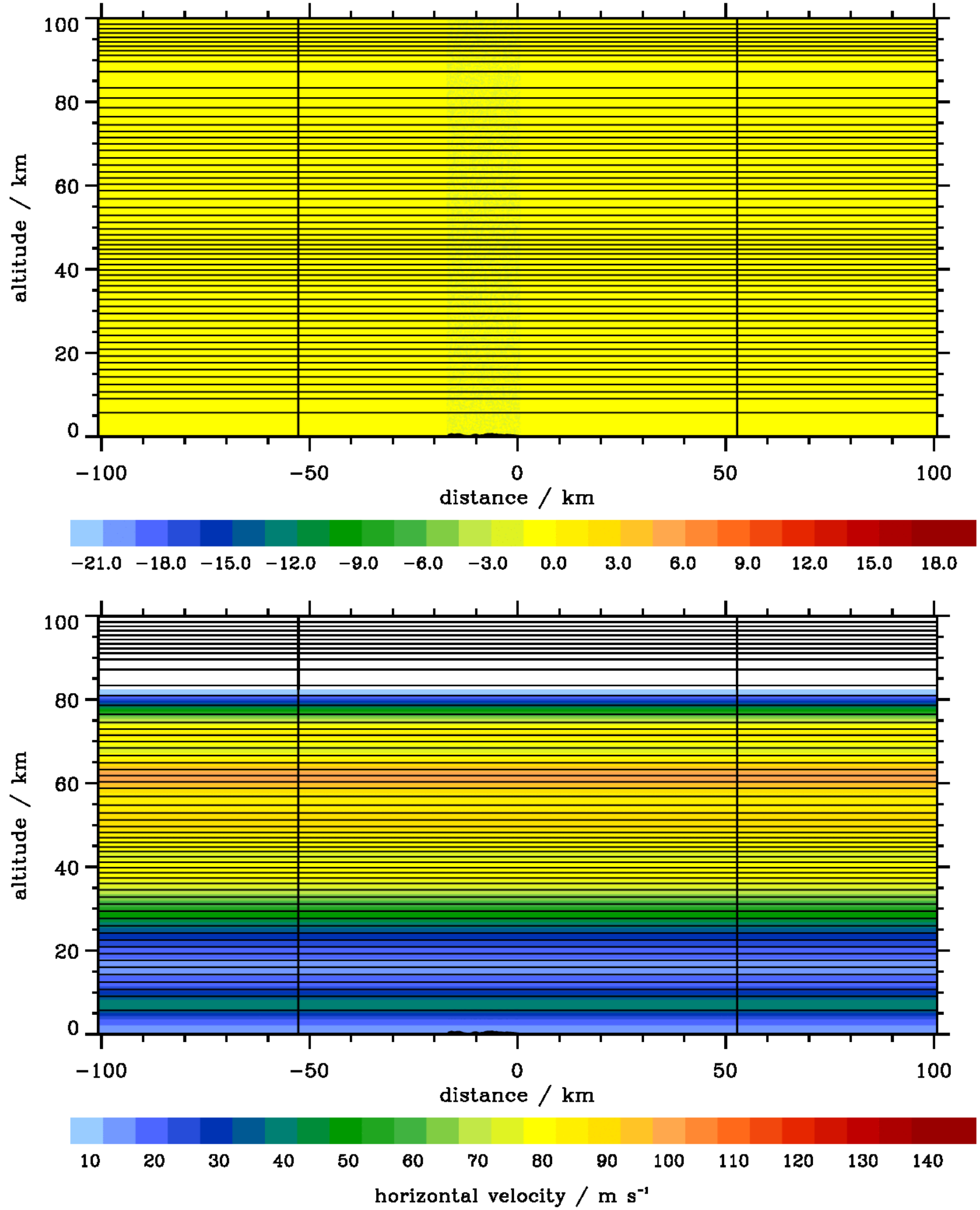

altitude / km
distance / km
−21.0 −18.0 −15.0 −12.0 −9.0 −6.0 −3.0 0.0 3.0 6.0 9.0 12.0 15.0 18.0
altitude / km
distance / km
10 20 30 40 50 60 70 80 90 100 110 120 130 140
horizontal velocity / m s⁻¹

t = 6 min

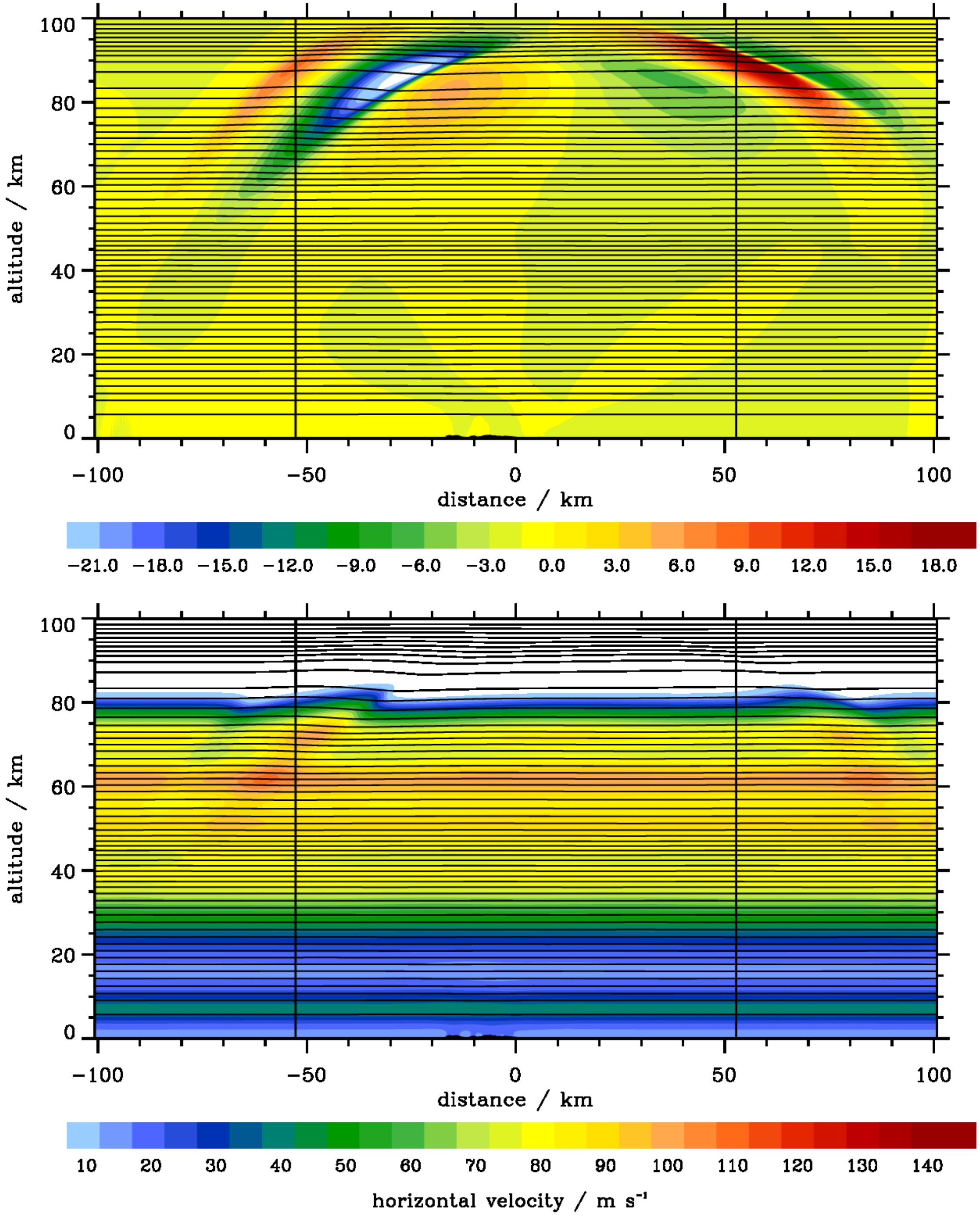
100
80
60
40
20
0
altitude / km
−100
−50
0
50
100
distance / km
−21.0 −18.0 −15.0 −12.0 −9.0 −6.0 −3.0 0.0 3.0 6.0 9.0 12.0 15.0 18.0
100
80
60
40
20
0
altitude / km
−100
−50
0
50
100
distance / km
10 20 30 40 50 60 70 80 90 100 110 120 130 140
horizontal velocity / m s⁻¹

t = 60 min

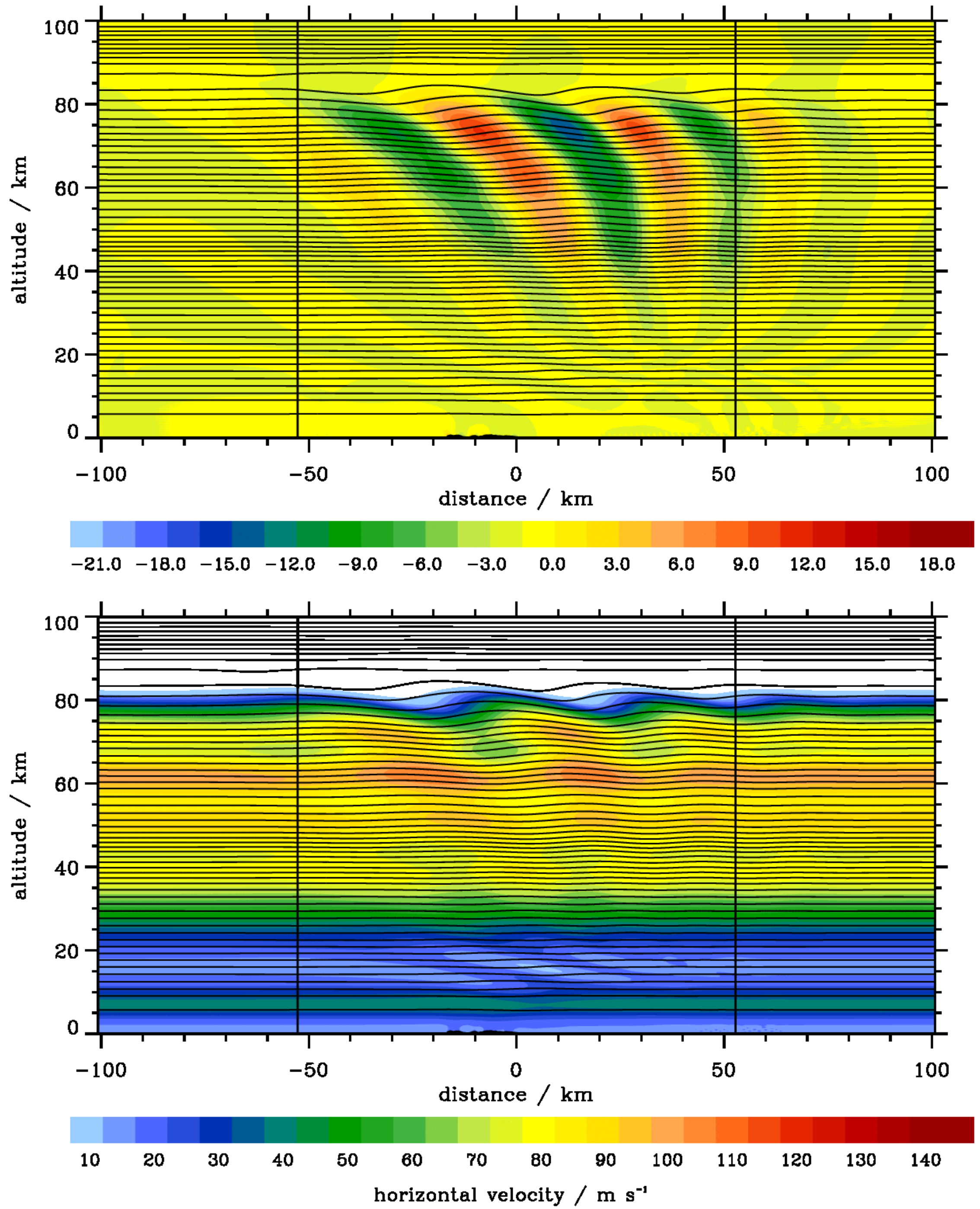

100
80
60
40
20
0
altitude / km
−100
−50
0
50
100
distance / km
−21.0 −18.0 −15.0 −12.0 −9.0 −6.0 −3.0 0.0 3.0 6.0 9.0 12.0 15.0 18.0
100
80
60
40
20
0
altitude / km
−100
−50
0
50
100
distance / km
10 20 30 40 50 60 70 80 90 100 110 120 130 140
horizontal velocity / m s⁻¹

t = 90 min

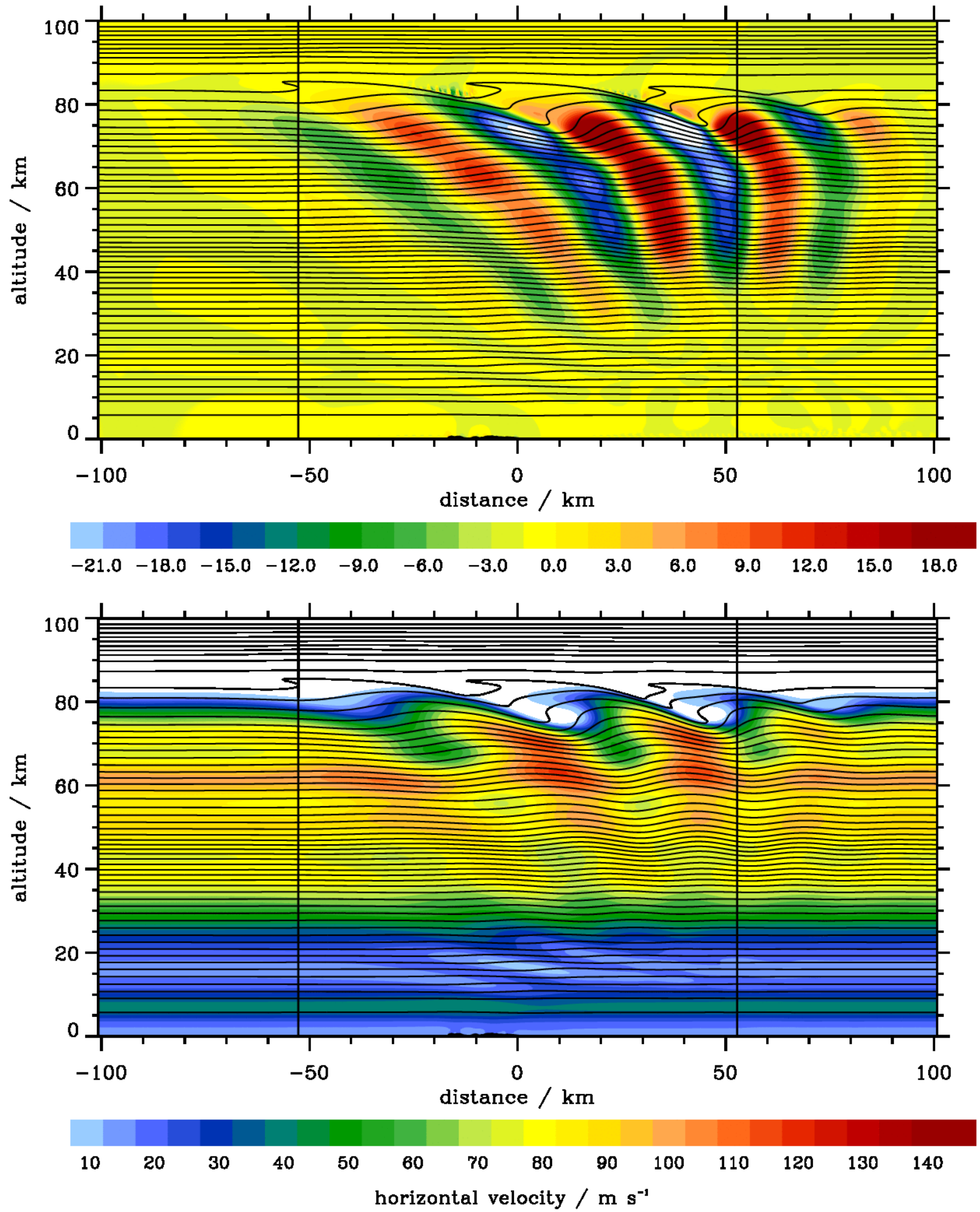

100
80
60
40
20
0
altitude / km
−100
−50
0
50
100
distance / km
−21.0
−18.0
−15.0
−12.0
−9.0
−6.0
−3.0
0.0
3.0
6.0
9.0
12.0
15.0
18.0
100
80
60
40
20
0
altitude / km
−100
−50
0
50
100
distance / km
10
20
30
40
50
60
70
80
90
100
110
120
130
140
horizontal velocity / m s⁻¹

t = 90 min

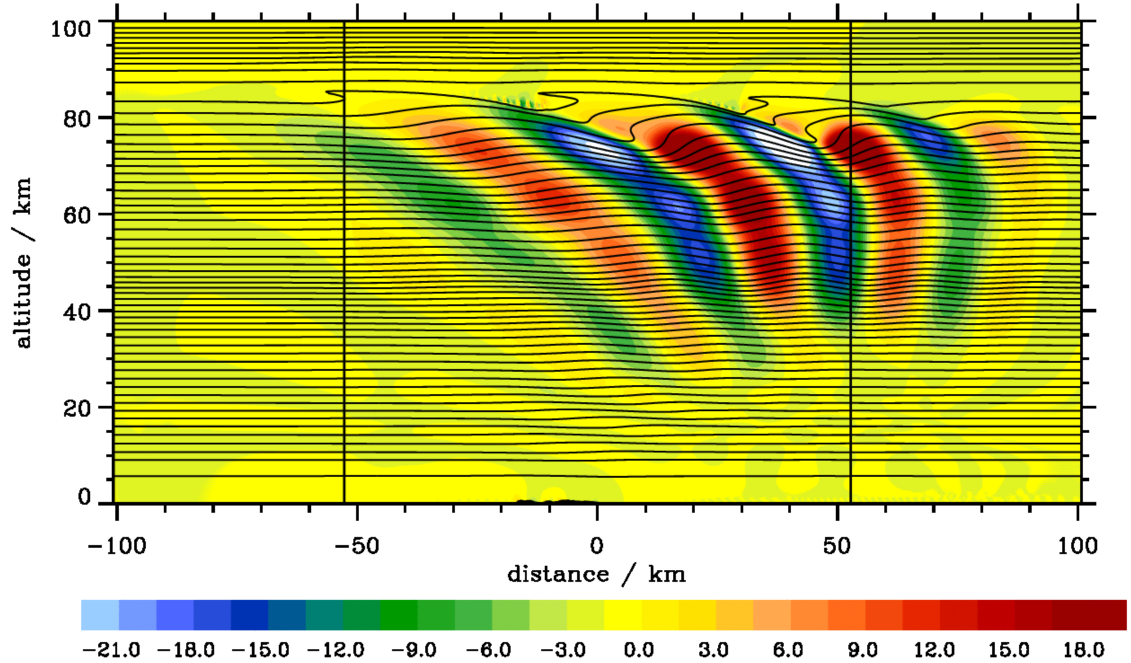

altitude / km
100
80
60
40
20
0
−100
−50
0
50
100
distance / km
−21.0
−18.0
−15.0
−12.0
−9.0
−6.0
−3.0
0.0
3.0
6.0
9.0
12.0
15.0
18.0

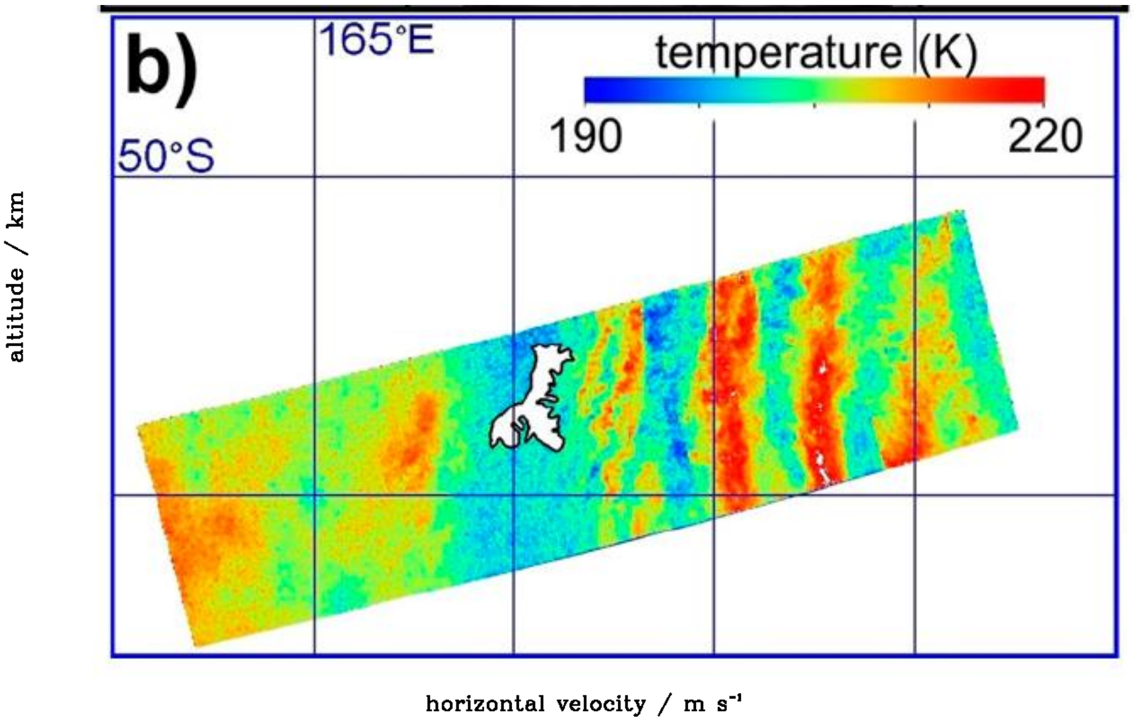

b)
165°E
50°S
temperature (K)
190
220
altitude / km
horizontal velocity / m s-1

t = 120 min

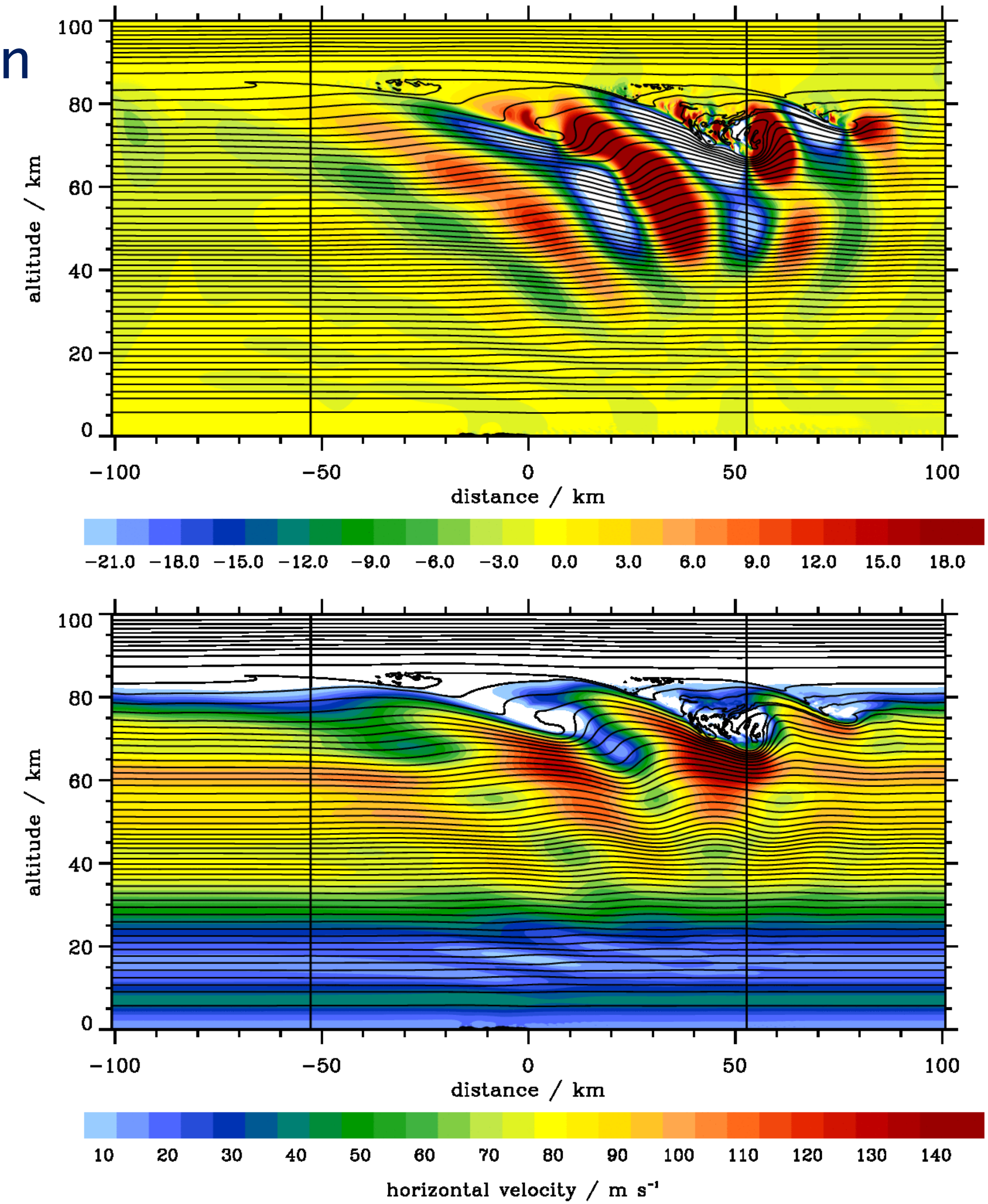

100
80
60
40
20
0
altitude / km
−100
−50
0
50
100
distance / km
−21.0 −18.0 −15.0 −12.0 −9.0 −6.0 −3.0 0.0 3.0 6.0 9.0 12.0 15.0 18.0
100
80
60
40
20
0
altitude / km
−100
−50
0
50
100
distance / km
10 20 30 40 50 60 70 80 90 100 110 120 130 140
horizontal velocity / m s⁻¹

Mesospheric Rotors

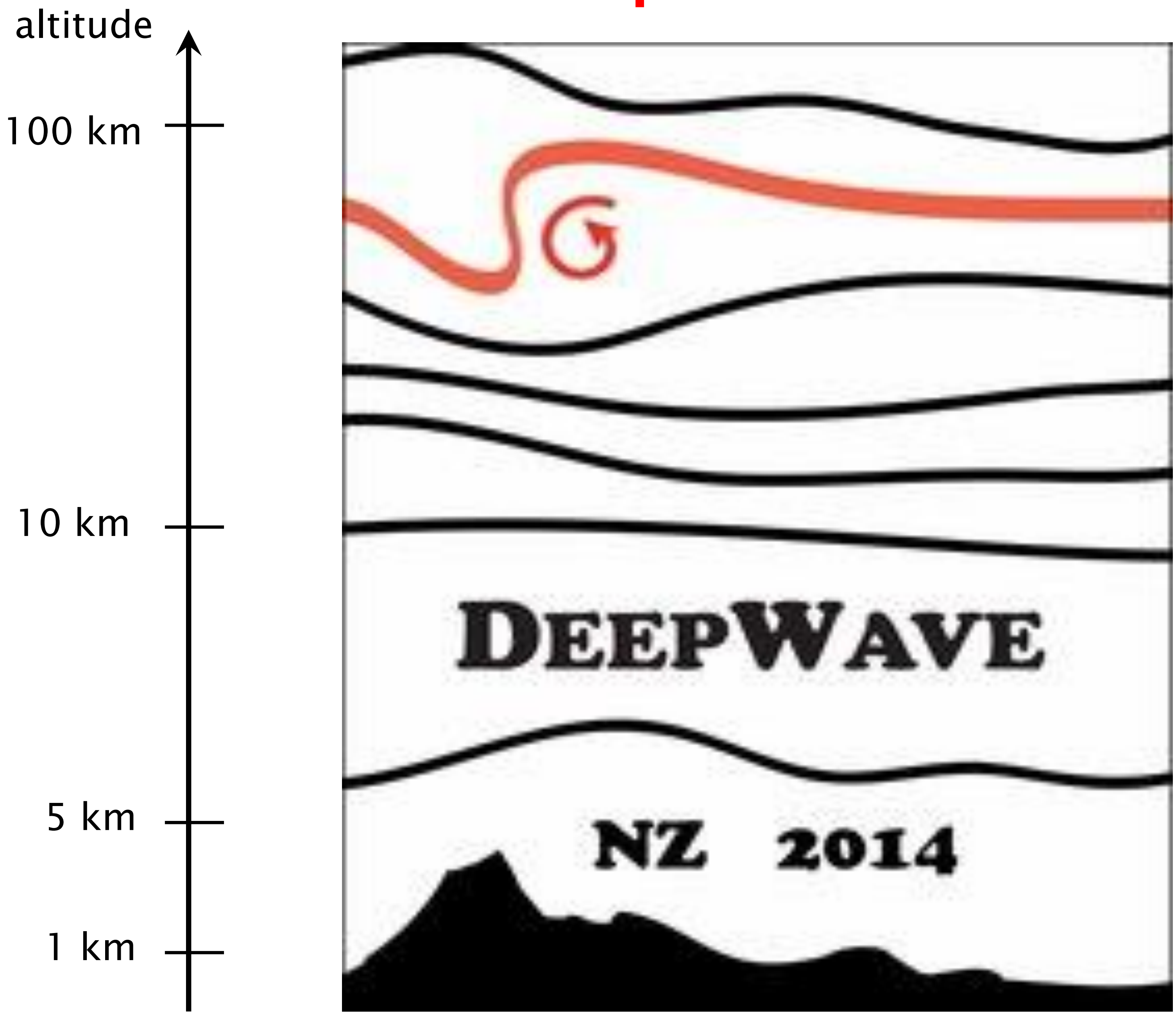

RF05 16 June 2014

- why RF05??

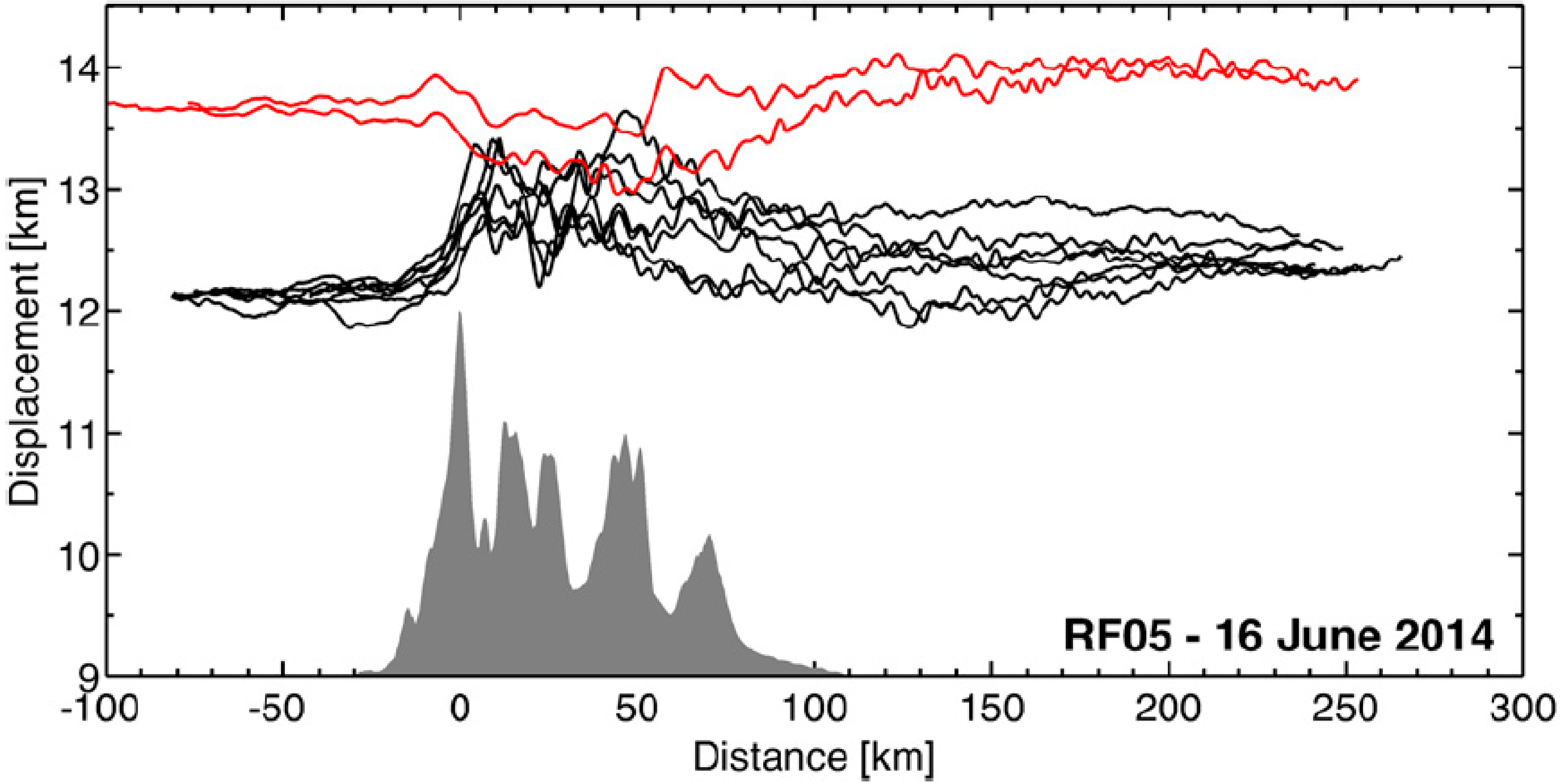

FIG. 8. Aircraft-derived patterns of vertical air displacement for nine legs over Mt. Cook during RF05 on 16 Jun 2015. Seven of the legs were flown at z = 12.1 km (black) and two at z = 13.7 km (red). Note the lack of disturbance upstream and the multiple scales in the wave field. The mountain is to scale but offset vertically. Airflow is from left to right.

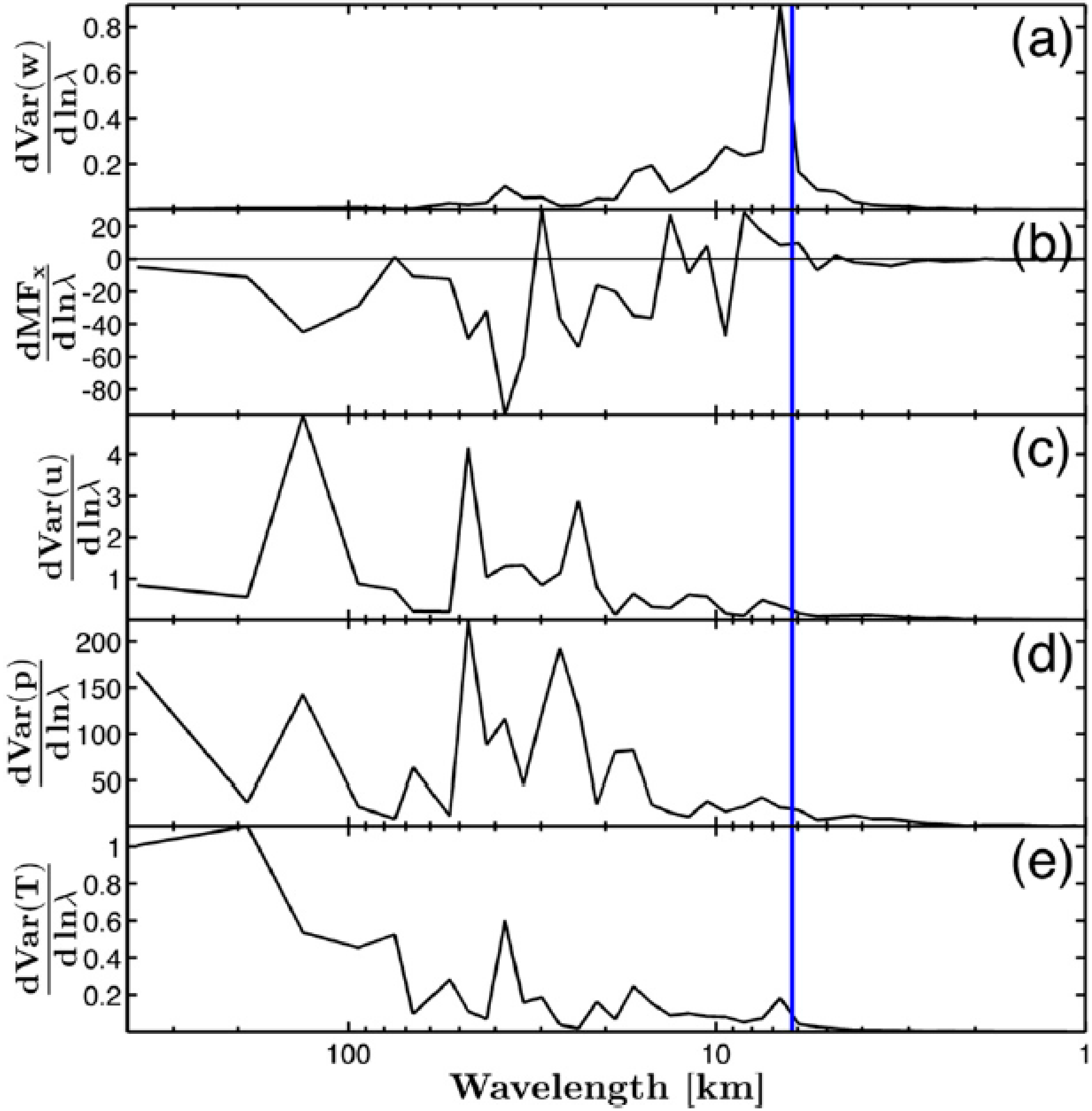

FIG. 9. Aircraft-derived spectra for Mt. Cook flight RF05, leg 11 on 16 Jun 2014: (a) w power, (b) MFx, (c) u power, (d) p power, and (e) T power. The vertical blue line is the estimated buoyancy cutoff for this leg. Note the shift in dominant wavelength between (a) and (c)–(e).

buoyancy cut-off wavelength

$$\lambda_C = 2\pi \frac{U}{N}$$

Observed waves over New Zealand have many characteristics of **steady linear mountain waves**

MAY 2017 SMITH AND KRUSE

TABLE 1. Four analyzed DEEPWAVE aircraft legs, all during 2014.

RF	Leg	Date	Mountain	Spectrum	U ($\mathrm{m\,s^{-1}}$)	Std dev (u'; $\mathrm{m\,s^{-1}}$)	λ_C (km)	Std dev (w'; $\mathrm{m\,s^{-1}}$)	EFz ($\mathrm{W\,m^{-2}}$)	MFx (mPa)
05	11	16 Jun	Cook	Broad	20	2.6	6.2	0.63	3.0	−94
08	7	20 Jun	Aspiring	Broad	30	2.8	9.4	0.57	2.2	−86
09	11	24 Jun	Cook	Broad	28	5.2	8.8	1.01	7.6	−110
16	1	4 Jul	Aspiring	Narrow	39	3.1	12.2	1.55	21.5	−550

(1) positive EF_z, negative MF_x

(2) small nonlinearity ratio (i.e., $|u'|/U \ll 1$)

(3) horizontal energy □ux vector (i.e., $EF_x = \langle p'u' \rangle$ and $EF_y = \langle p'v' \rangle$) was oriented into the mean wind

(4) Eliassen-Palm relationship EF_z = -**U·MF** was well satis□ed

(5) w-power dominated by the shorter waves, u-power dominated by the longer waves. EF_z and MF_x : contributions from both wave scales, with the short waves dominating in the stronger events

RF05 16 June 2014

- why RF05??

(1) Smith & Kruse (2017) show observed broad spectra but no simulations – „… one of the most rugged terrains in the world. Small-scale relief exceeds 1 km in the high mountain areas (Korup et al. 2005). This roughness broadens the terrain spectrum and the associated wave spectra found in the atmosphere."

Is the rougged terrain alone responsible for the broad spectra? Are these short waves observational artifacts? Do we understand their origins?

RF05 16 June 2014

- why RF05??

(2) GV-Summary (by Ron): „ …The pattern of waves across the island was very repeatable leg after leg. Near 170E, the UIC drops from about 20m/s to 10m/s, slight turbulence is found and short wave train begins. Typical amplitude of the vertical velocity in the wave train was 2 m/s. The wavelength was about 10km. It extends usually all the way to the east end of the leg. It is the longest wave oscillation I have ever seen on the atmosphere with about 30 full oscillations. Over the ridge crest, there were longer non-periodic waves that were probably vertically propagating. …"

EULAG Simulations

- initial/background profiles: ECMWF upstream profiles 06, 07, …., 13 UTC
- inviscid, compressible runs
- dx=500 m, dz=200 m, dt=0.5 s
- simulation time 12 h
- smooth and rough topographies of Mt Cook 1b
- ongoing: sensitivity studies (absorber, Rayleigh damping time scale, resolution, set of equations, vertical coordinate transformations, …)

ECMWF IFS Upstream Profiles 16 June 2016 12 UTC

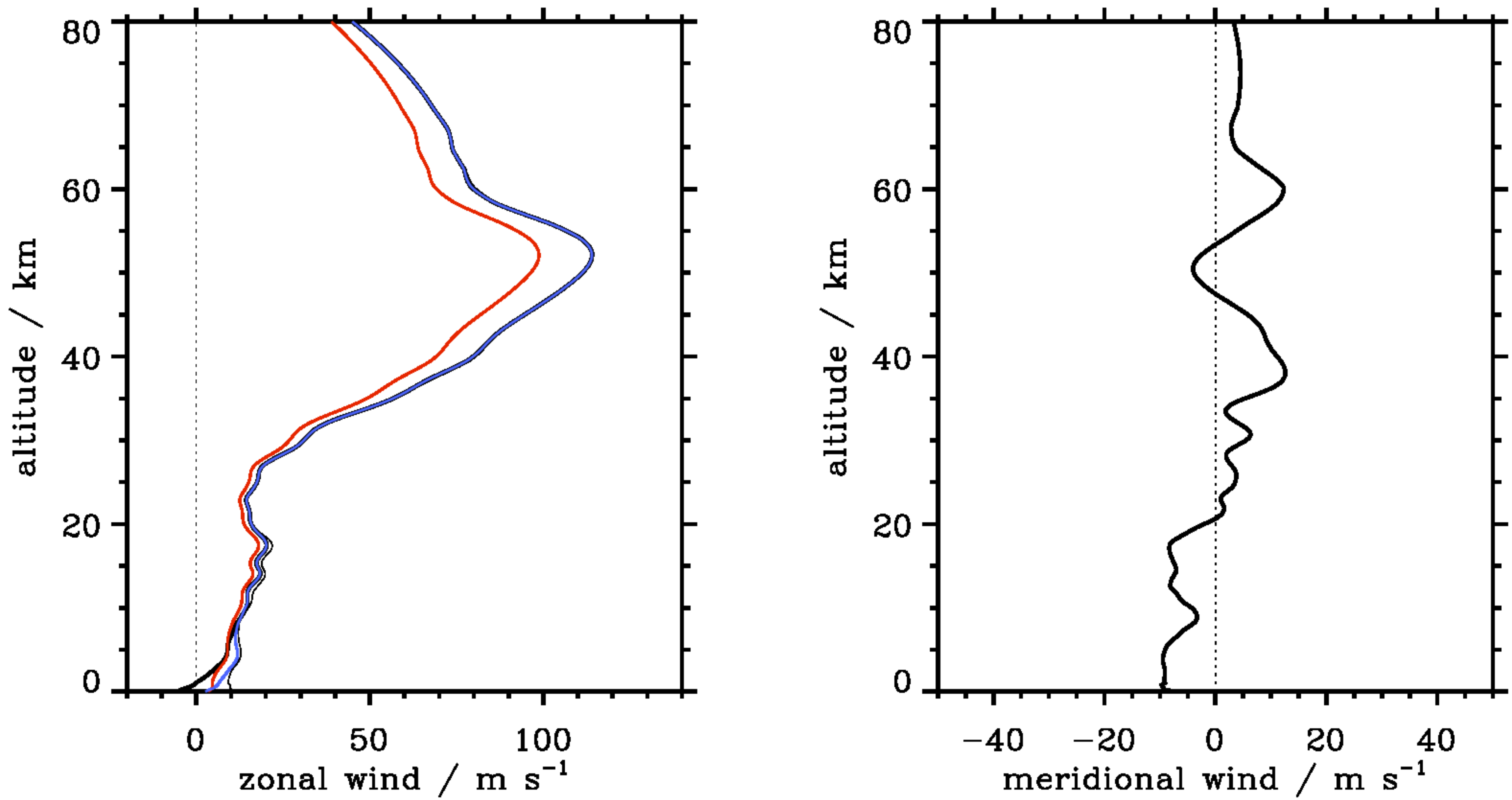

thick black line: u   **red line**: u_{ROT1} (magnitude of positive $u_{\parallel}$ and $v_{\parallel}$ with 300˚ along track direction)

thin black line: v_H **blue line**: u_{ROT2} (wind direction turns from 320˚ to 270˚ in the lowest 10 km)

ECMWF IFS Upstream Profiles 16 June 2016 12 UTC

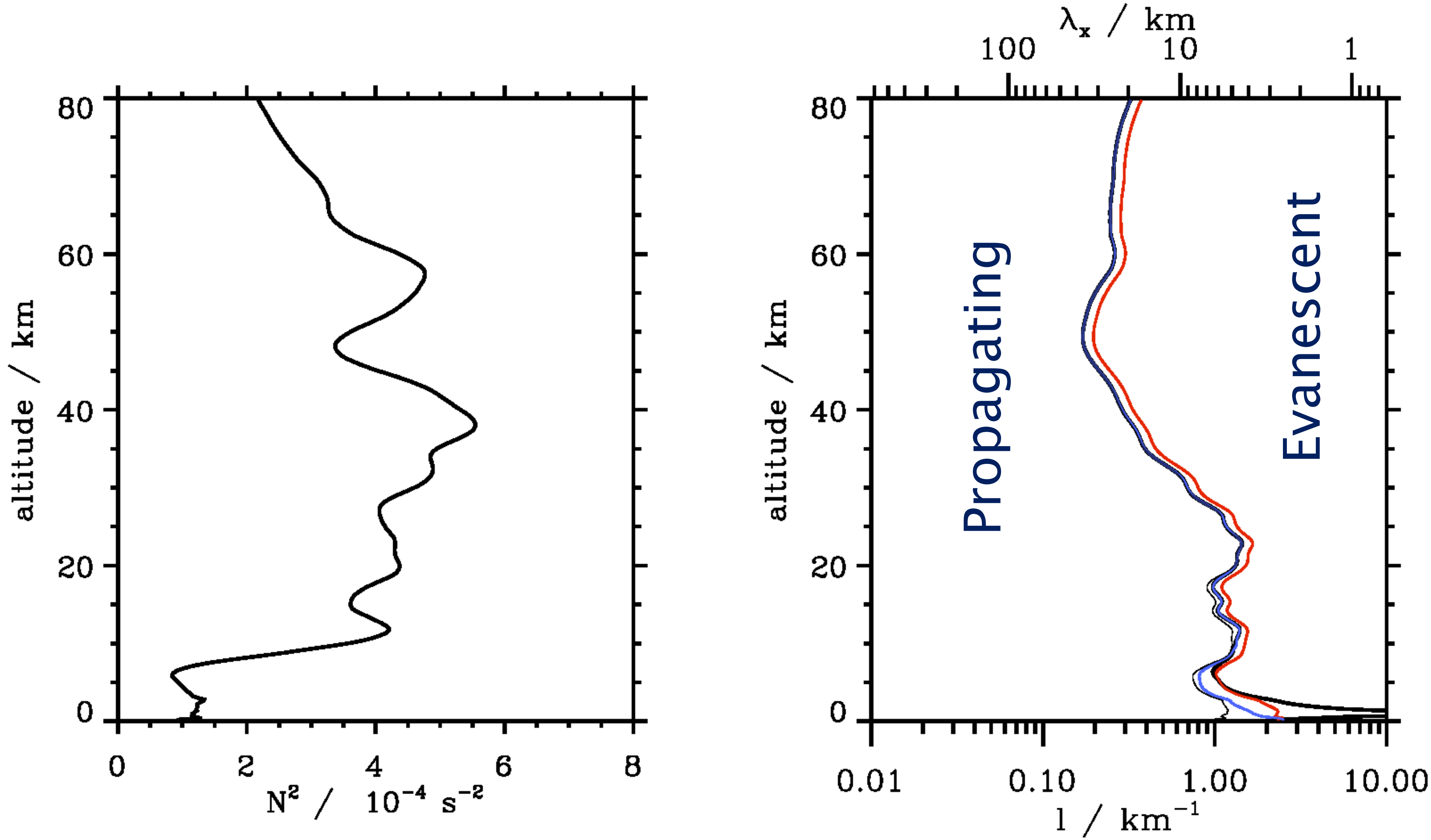

thick black line: u **red line**: u_{ROT1} (magnitude of positive $u_\parallel$ and $v_\parallel$ with 300° along track direction)

thin black line: v_H **blue line**: u_{ROT2} (wind direction turns from 320° to 270° in the lowest 10 km)

EULAG u-field every 360 s for 12 h started at 16 June 2016 12 UTC

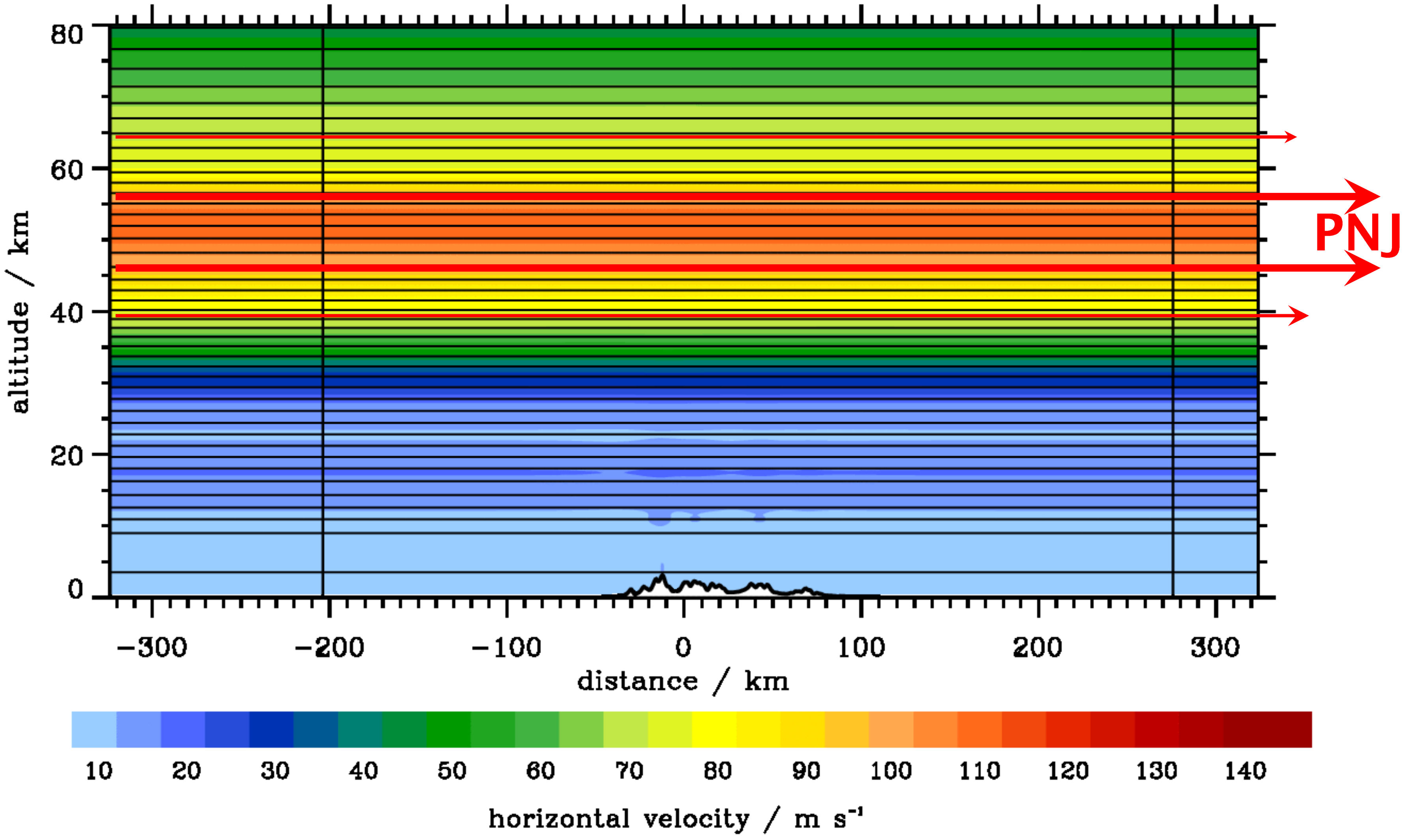

t = 90 min – excitation of stratospheric wave trains

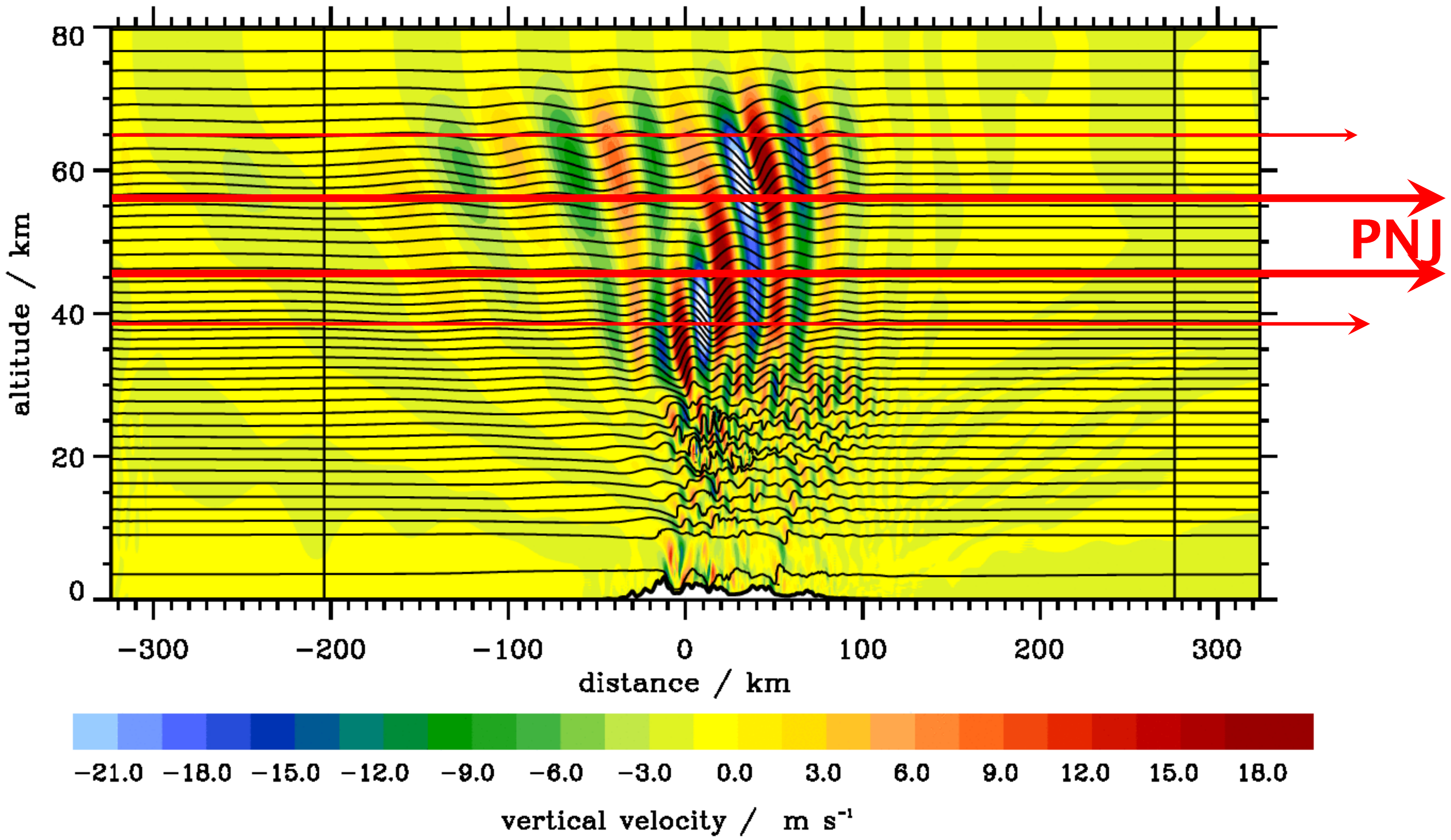

t = 90 min – excitation of stratospheric wave trains

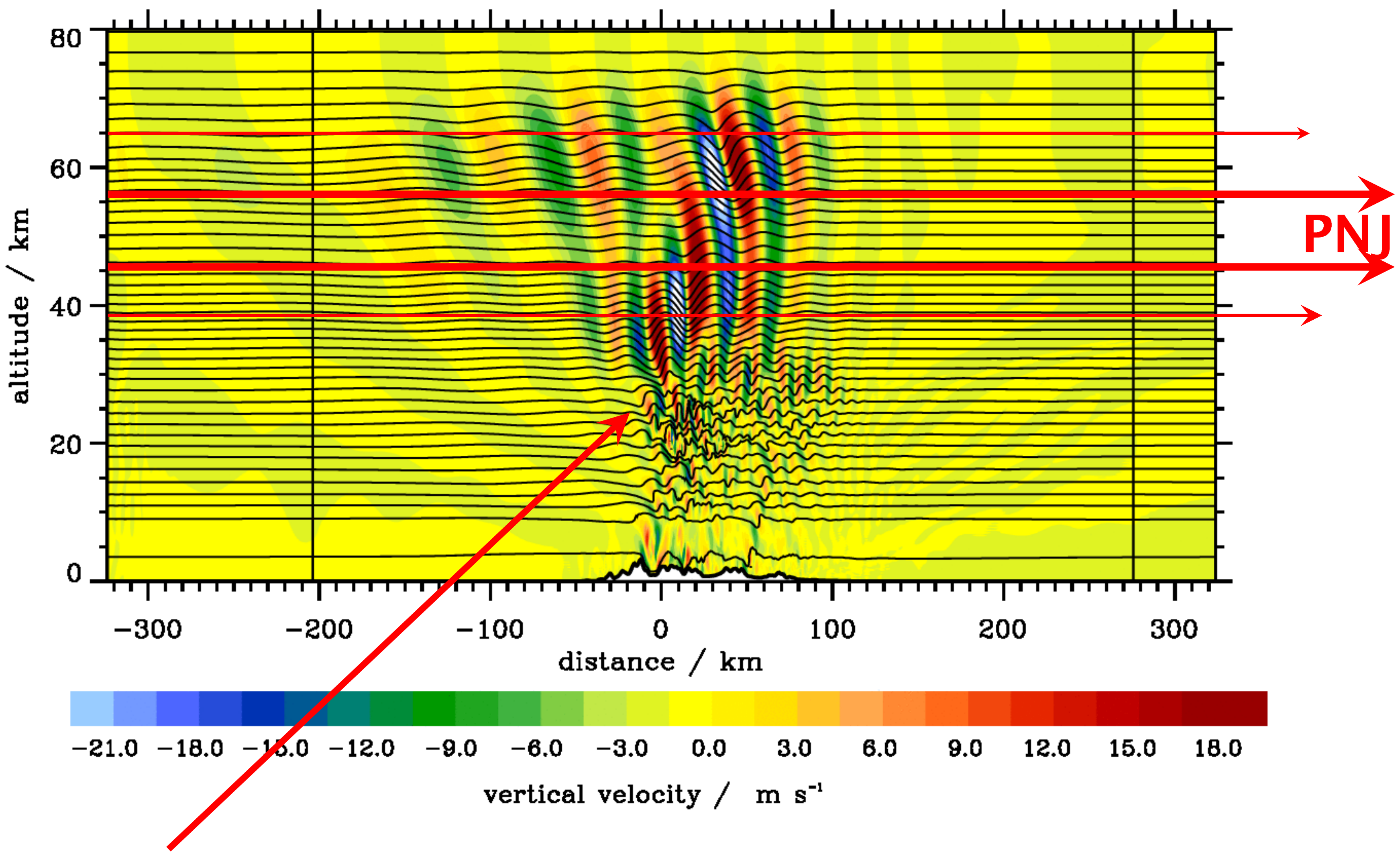

primary breaking region

t = 90 min – excitation of stratospheric wave trains

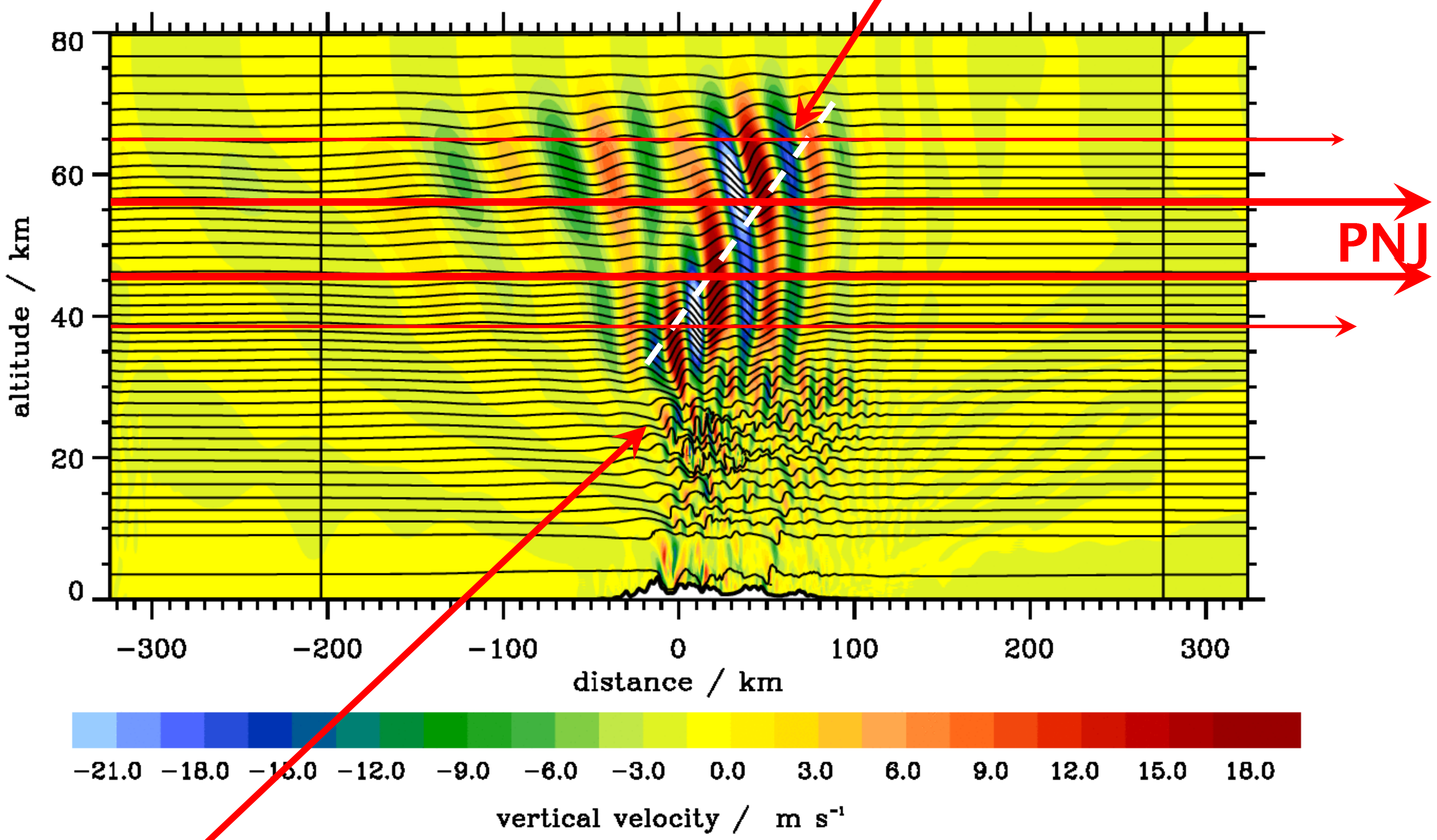

primary breaking region

t = 90 min – excitation of stratospheric wave trains

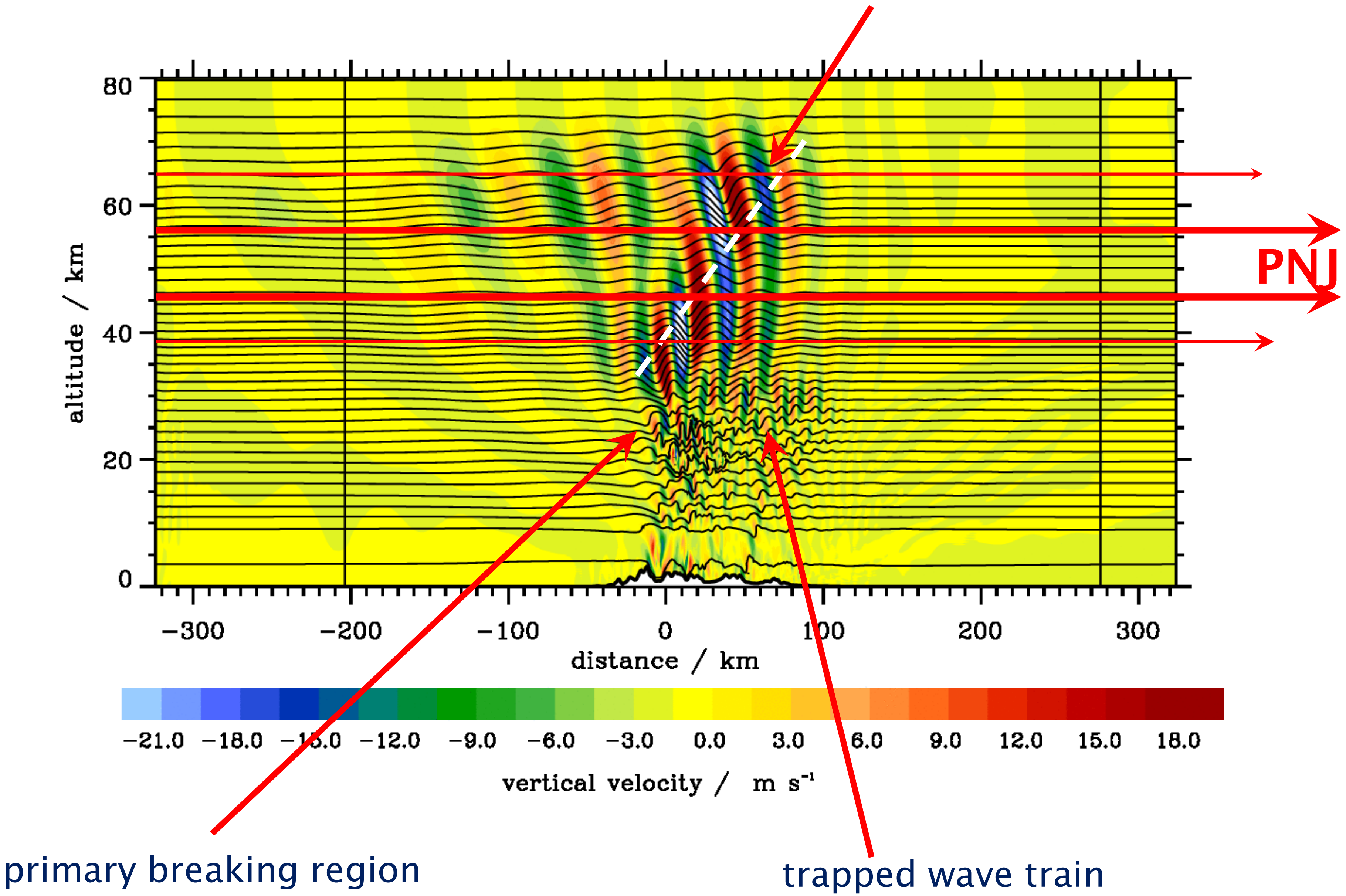

t = 138 min – ceased, almost linear stratospheric wave field

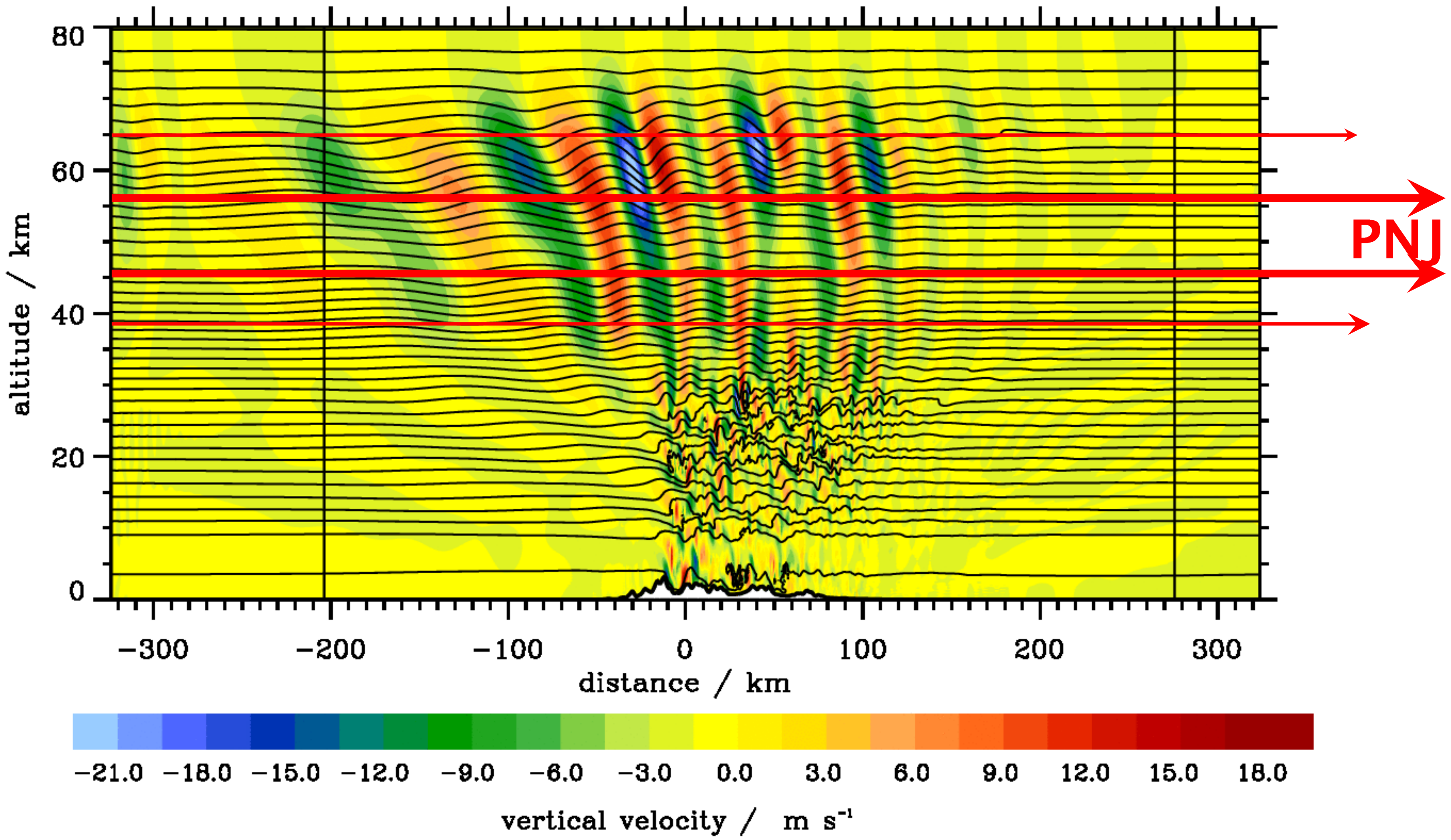

t = 540 min – sporadic appearance of mesospheric rotors

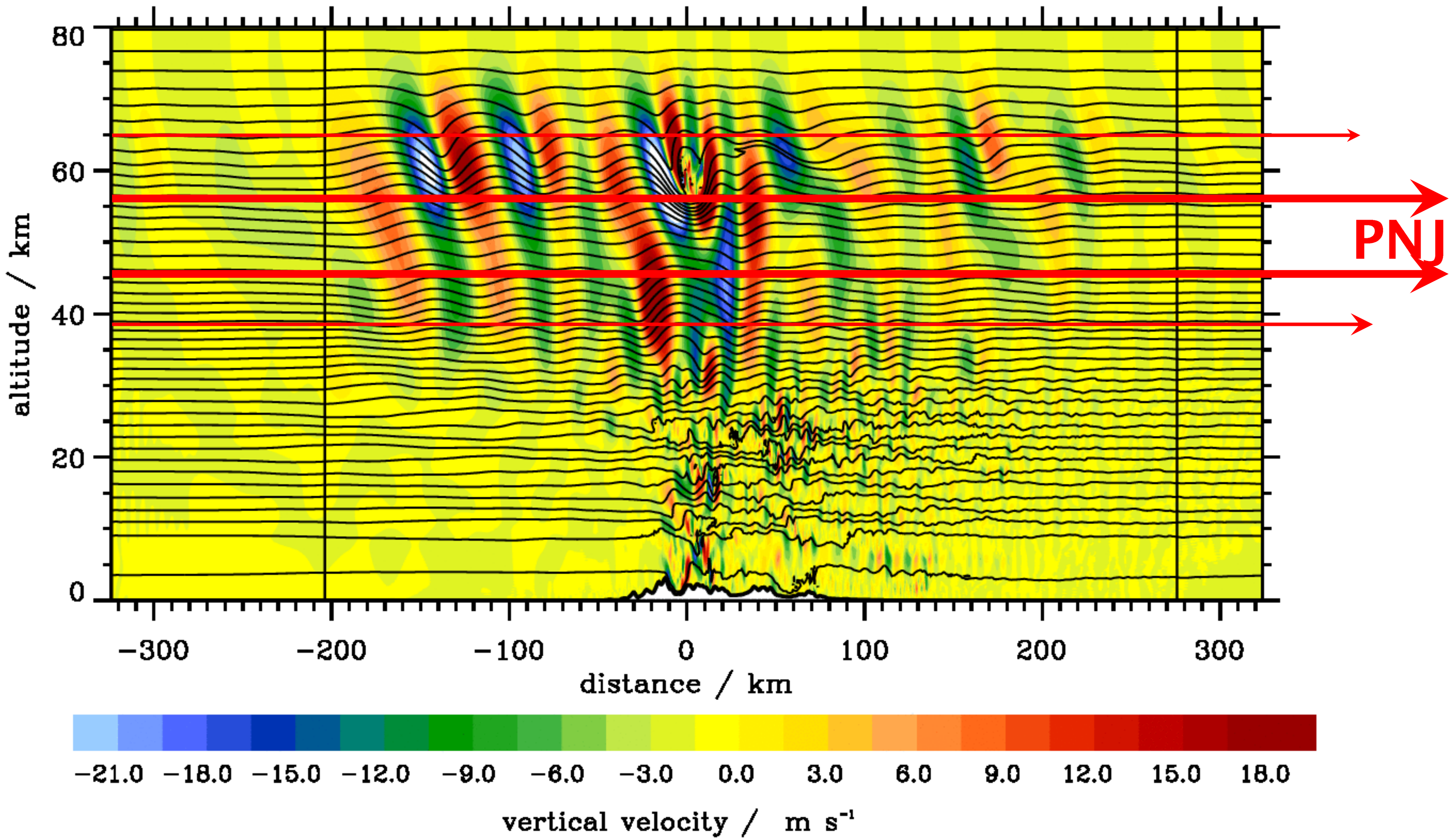

Prusa et al 1989 Bacmeister and Schoeberl 1989

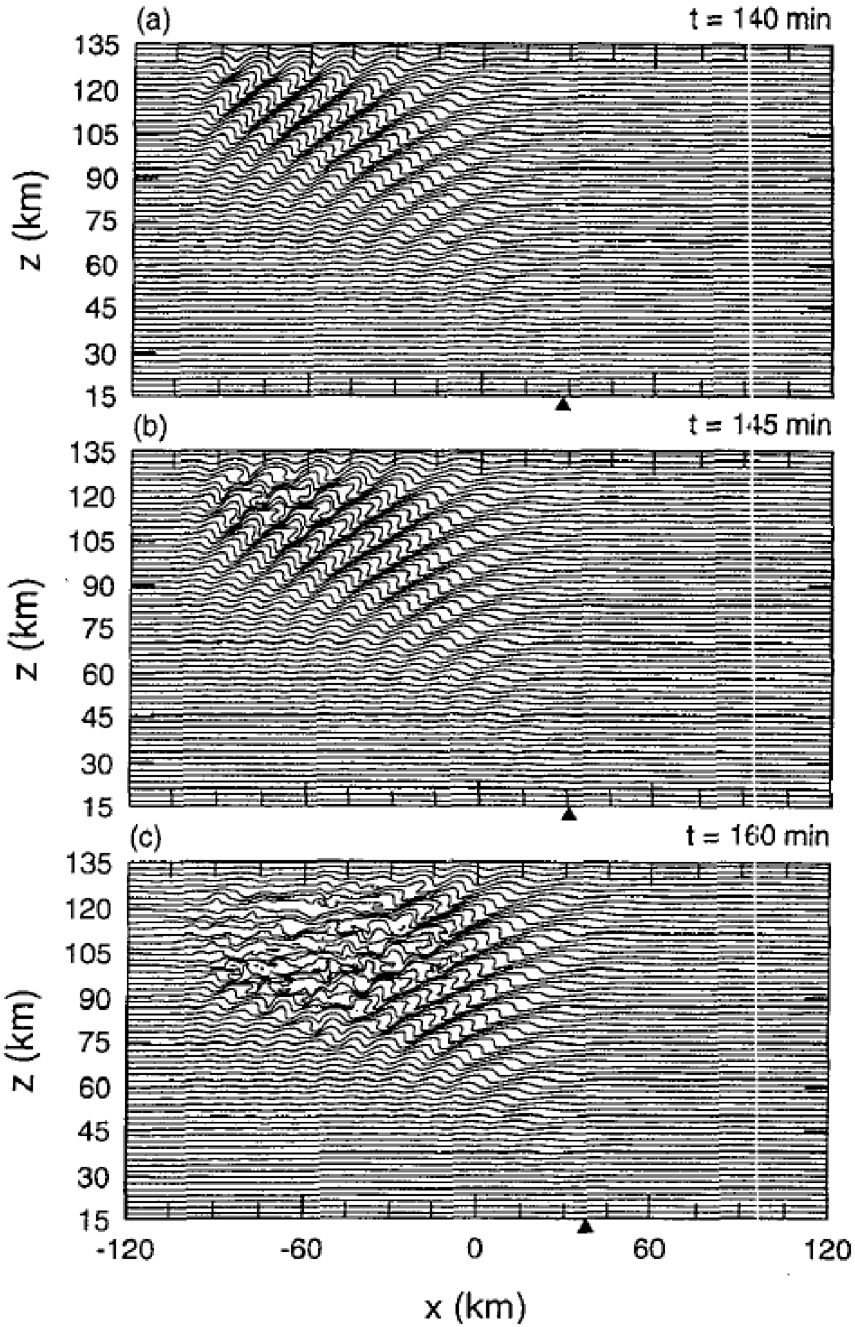

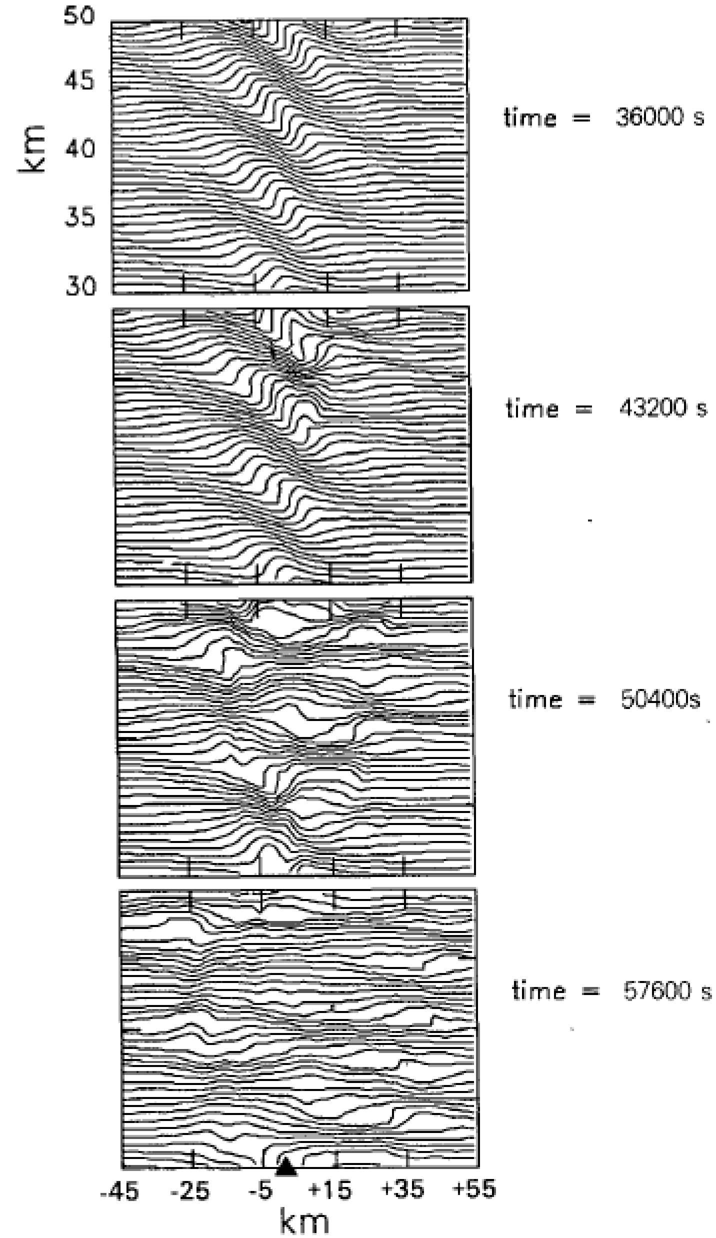

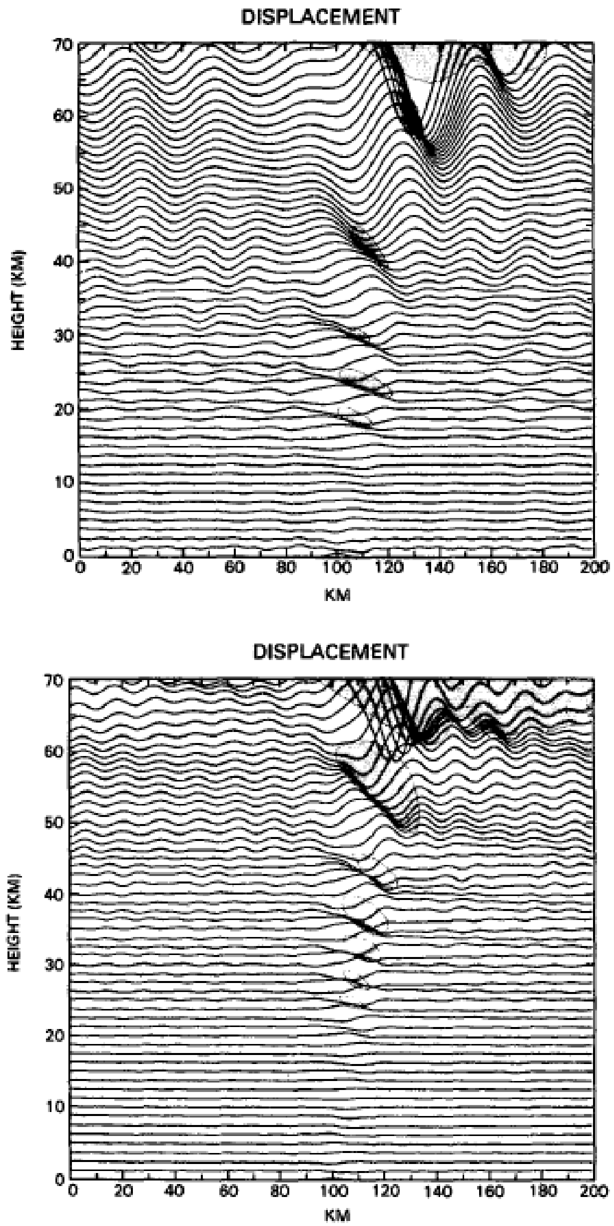

FIG. 2. Particle displacements associated with mountain waves are shown at different altitudes. The mountain is centered at 100 km and is profiled by the lowest displacement line. Panel (a), shows results using the winter wind profile; panel (b), the equinox wind profile. Shaded regions indicate zones where Ri < 1/4.

Schoeberl, M., 1985: The penetration of mountain waves into the middle atmosphere, *J. Atmos. Sci.* **42**, 2856-2864

Dynamics in the upper stratosphere and mesosphere

Internal Reflection of gravity waves

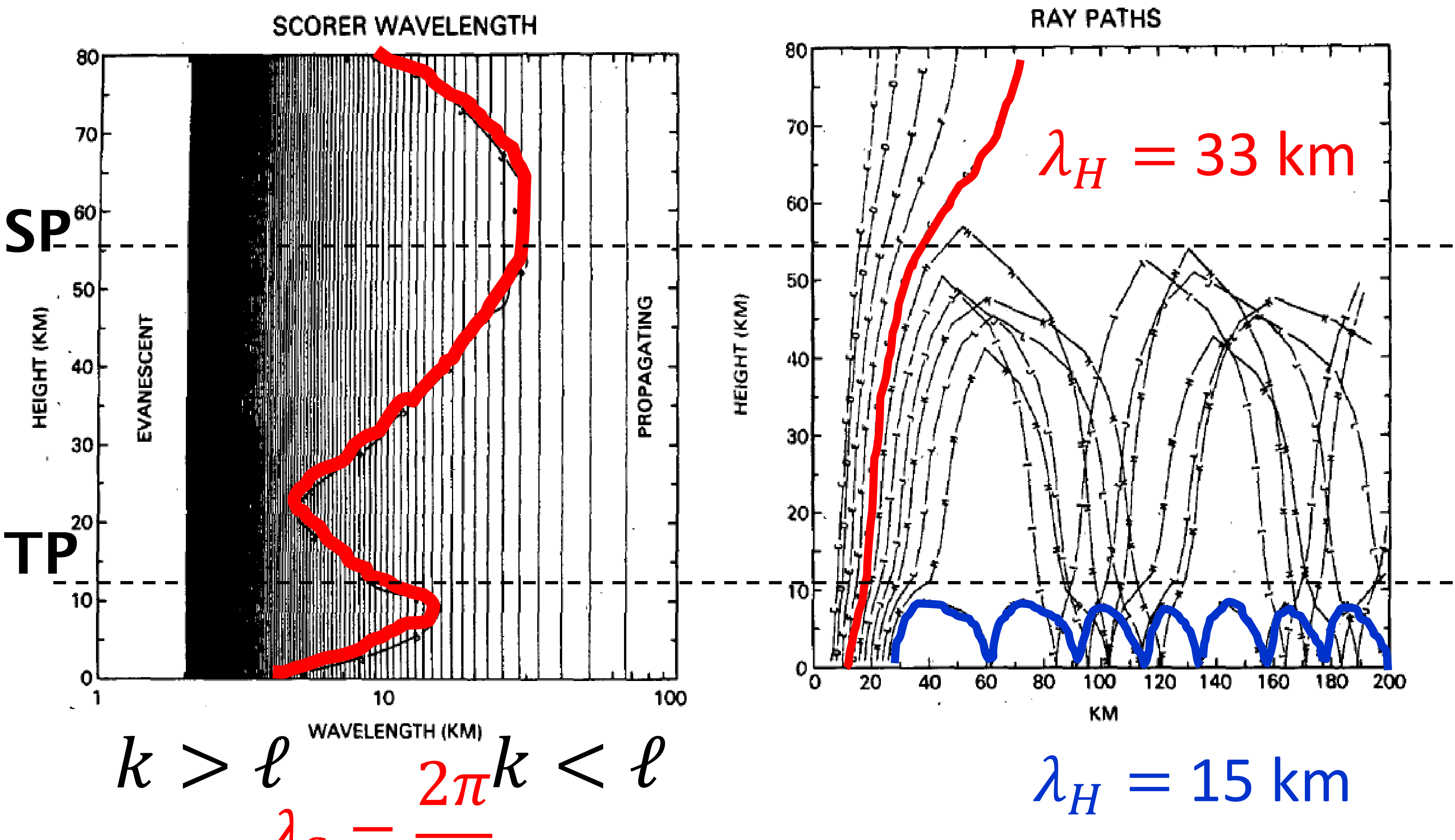

Schoeberl, 1985

Dynamics in the upper stratosphere and mesosphere

- deep vertical propagation of non-hydrostatic gravity waves

- waves trapped in the vicinity of the polar night jet (PNJ) and underneath the stratopause – <u>totally different appearance of wave fronts compared to uniform wind & uniform stability simulations</u>

- horizontally and vertically propagating waves above the PNJ

- sporadic wave breaking between strong up- and downdrafts (mesopheric rotors)

- very rapid change of middle atmospheric wave field in 12 h simulation time

Dynamics in the upper troposphere and lower stratosphere (UTLS)

- analyse rough and smoothed Mt. Cook 1b topography runs:
- show power spectra of u, w, and T at z=12 km along leg 11 of RF05 at one selected time

ECMWF IFS Upstream Profiles 16 June 2016 12 UTC

$\lambda_C = 2\pi \frac{U}{N}$

$\lambda_C = 2\pi \frac{U}{N}$

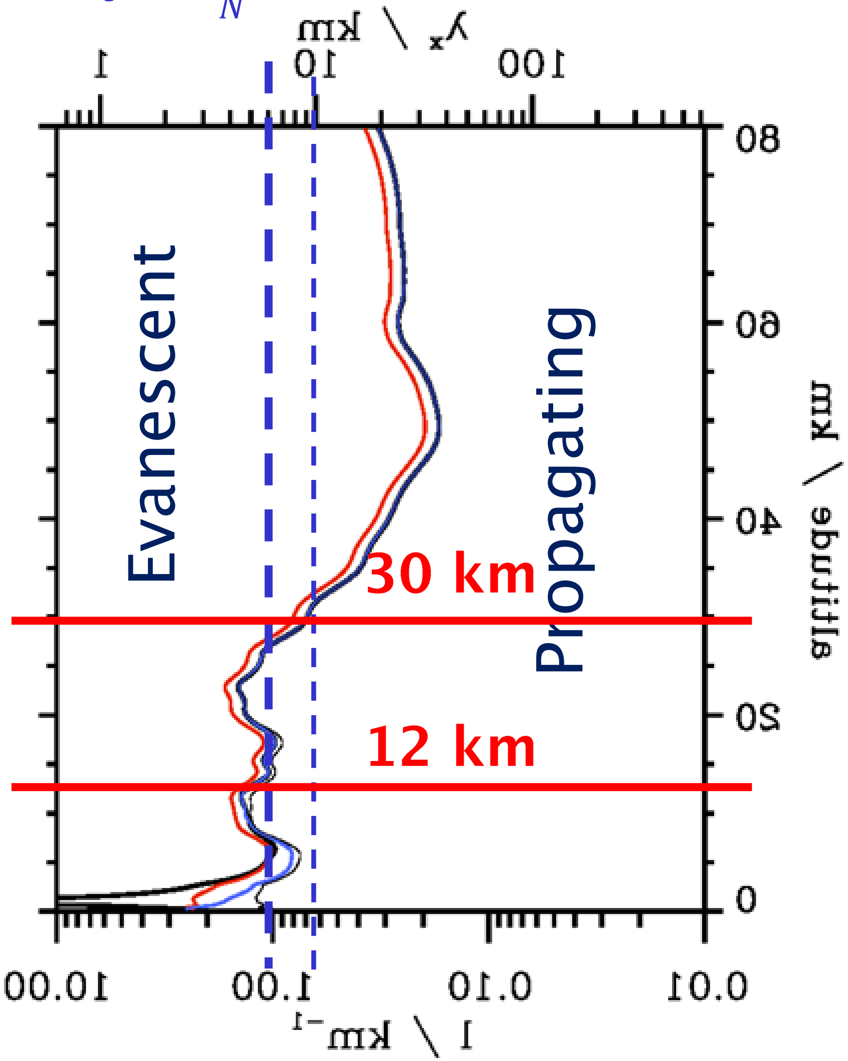

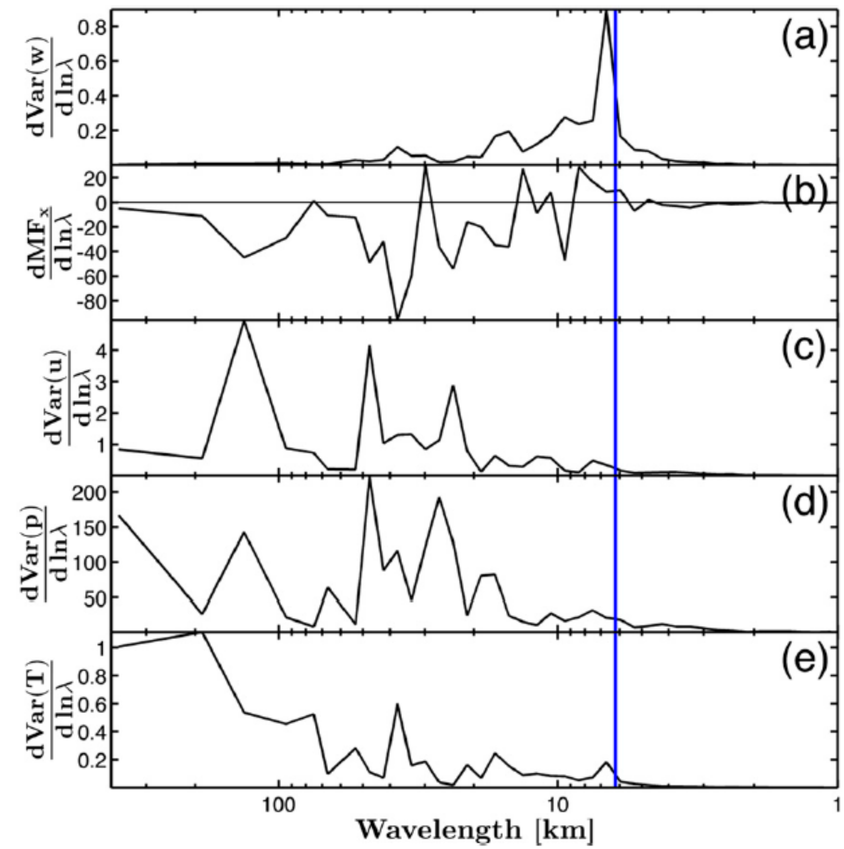

FIG. 9. Aircraft-derived spectra for Mt. Cook flight RF05, leg 11 on 16 Jun 2014: (a) w power, (b) MFx, (c) u power, (d) p power, and (e) T power. The vertical blue line is the estimated buoyancy cutoff for this leg. Note the shift in dominant wavelength between (a) and (c)–(e).

thick black line: u   **red line**: u_{ROT1} (magnitude of positive $u_{\parallel}$ and $v_{\parallel}$ with 300˚ along track direction)

thin black line: v_H **blue line**: u_{ROT2} (wind direction turns from 320˚ to 270˚ in the lowest 10 km)

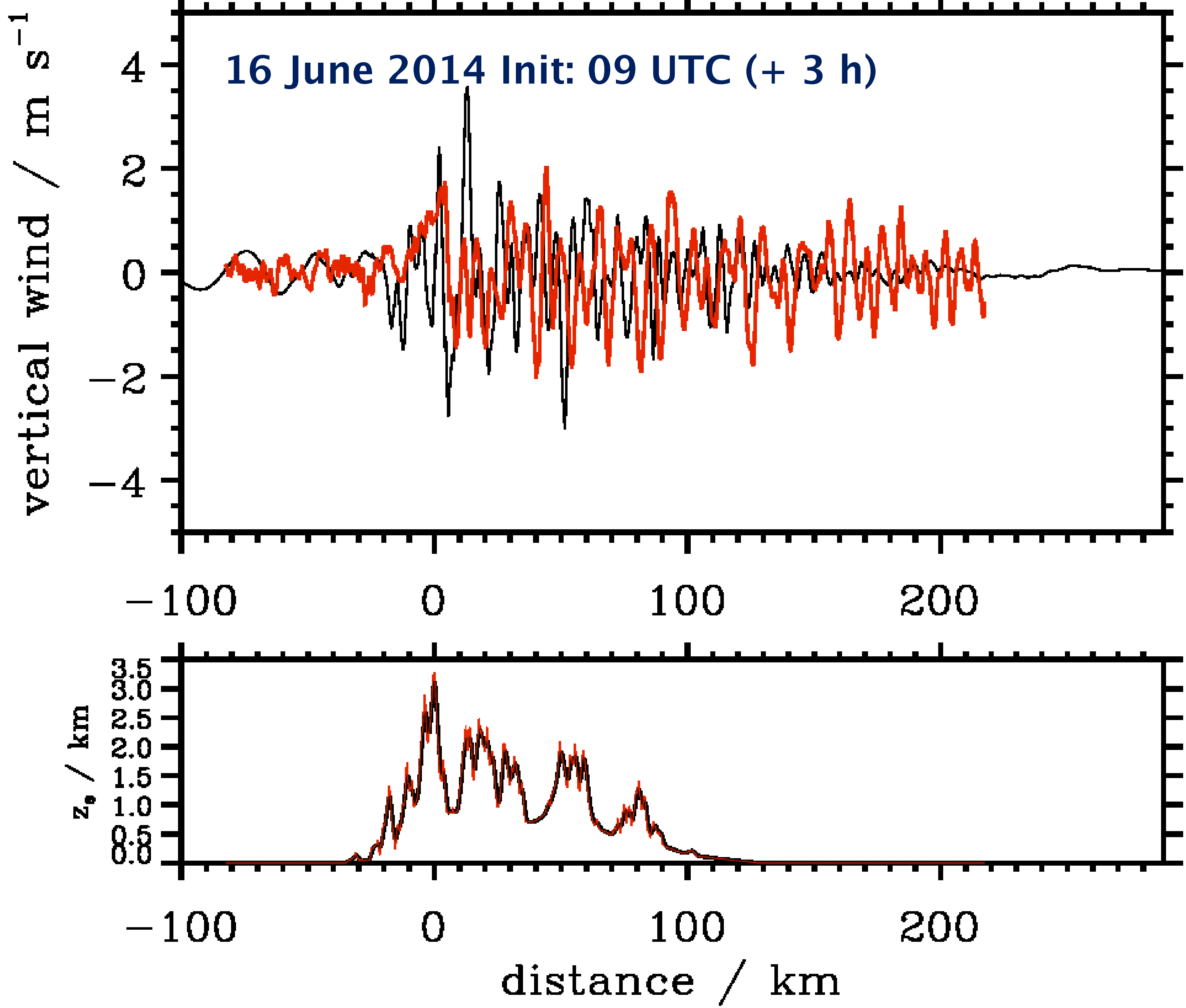
16 June 2014 Init: 09 UTC (+ 3 h)
vertical wind / m s^{-1}
4
2
0
−2
−4
−100
0
100
200
z_s / km
3.5
3.0
2.5
2.0
1.5
1.0
0.5
0.0
−100
0
100
200
distance / km

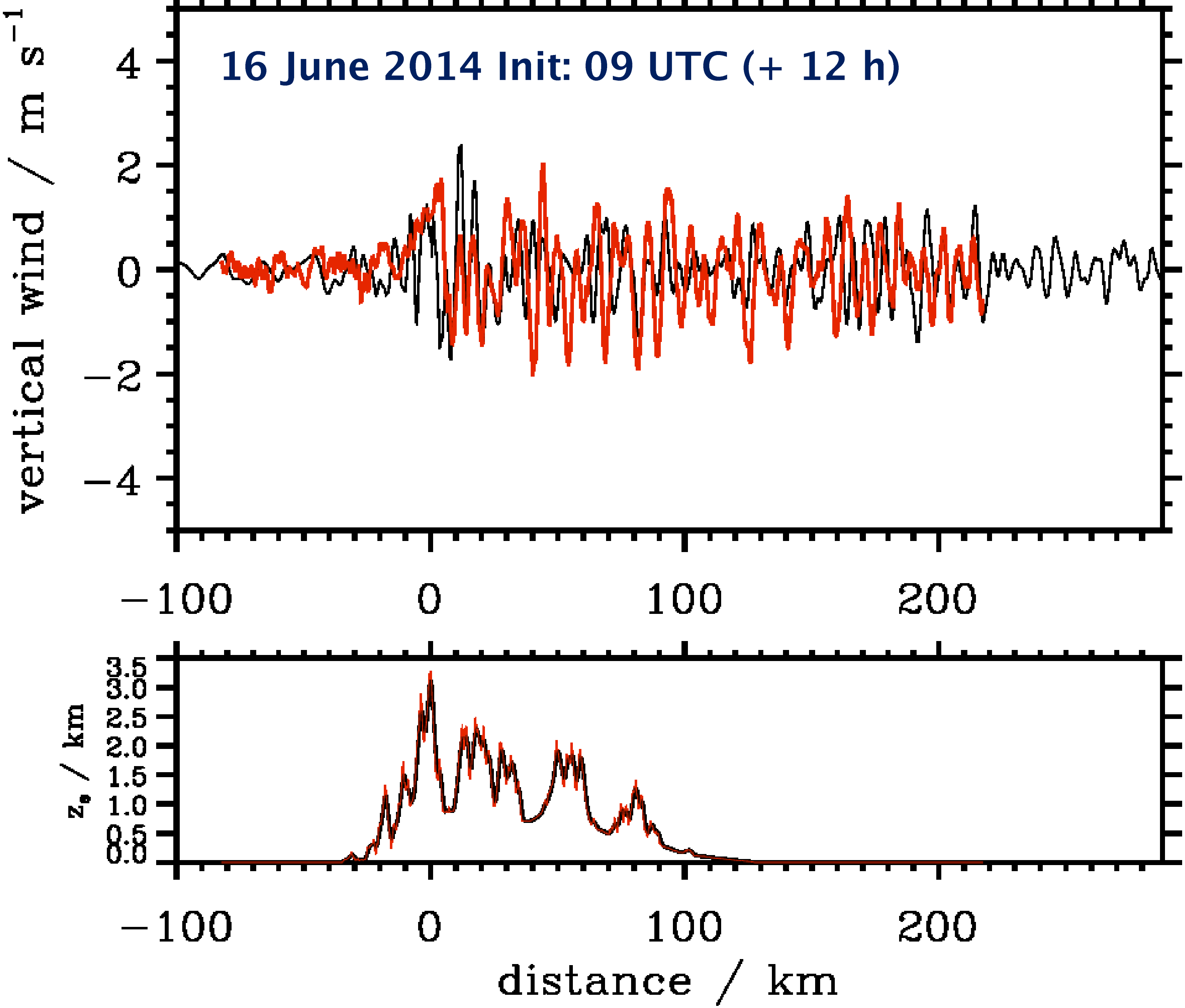
16 June 2014 Init: 09 UTC (+ 12 h)
vertical wind / m s^{-1}
4
2
0
−2
−4
−100
0
100
200
z_s / km
3.5
3.0
2.5
2.0
1.5
1.0
0.5
0.0
−100
0
100
200
distance / km

16 June 2016, Init: 12 UTC (+420 min)

z = 12 km

Mt Cook 1b – Rough EULAG run

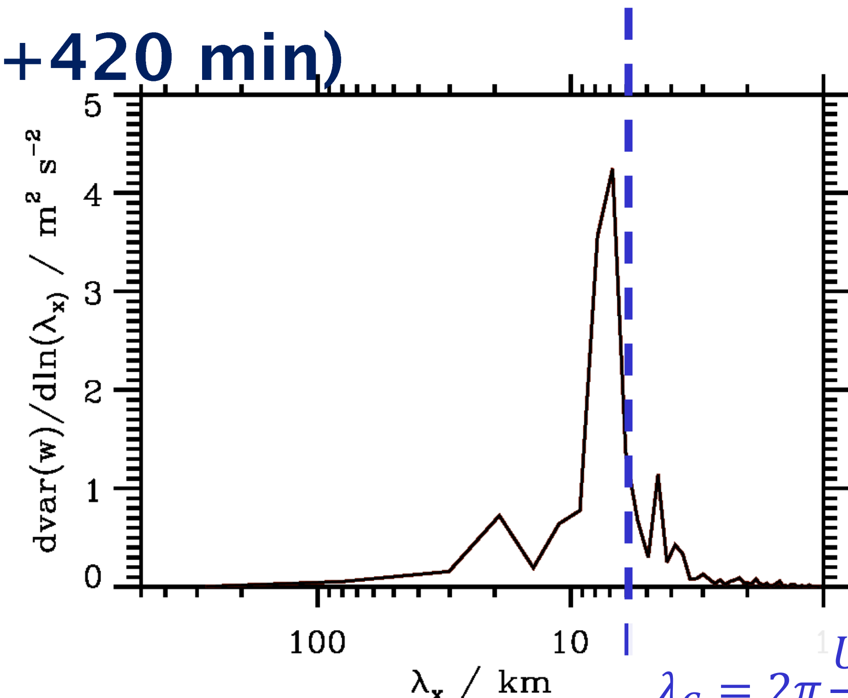

$$\lambda_C = 2\pi \frac{U}{N}$$

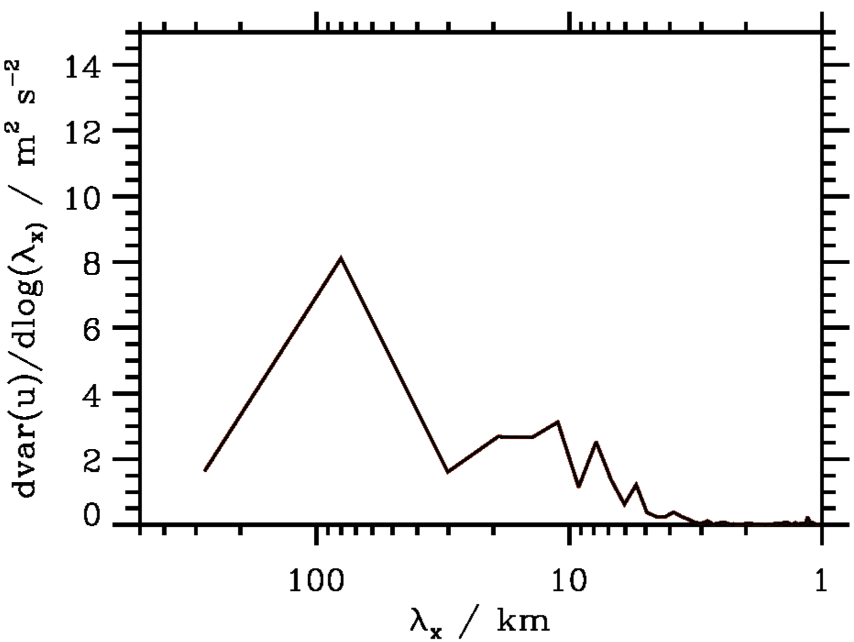

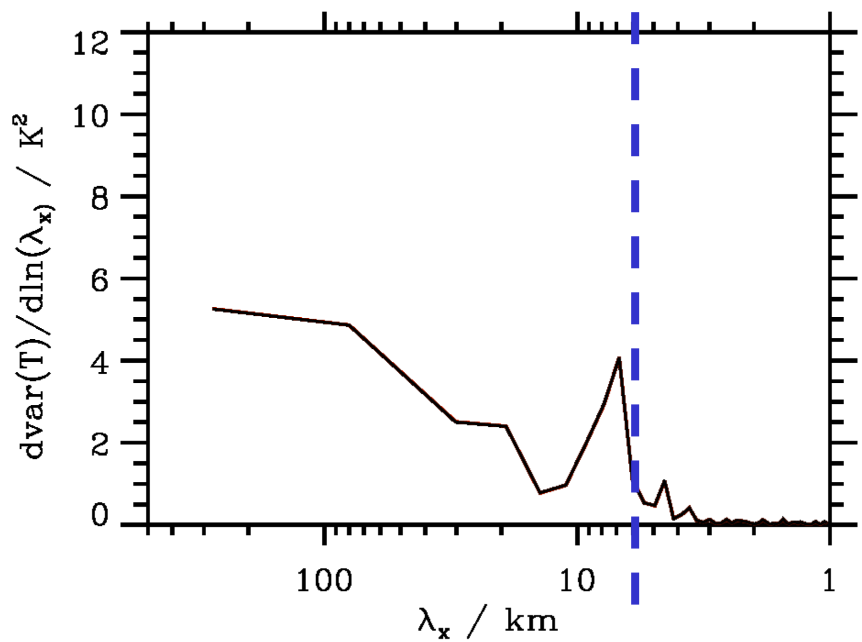

16 June 2016, Init: 12 UTC (+420 min)

z = 30 km

Mt Cook 1b – Rough EULAG run

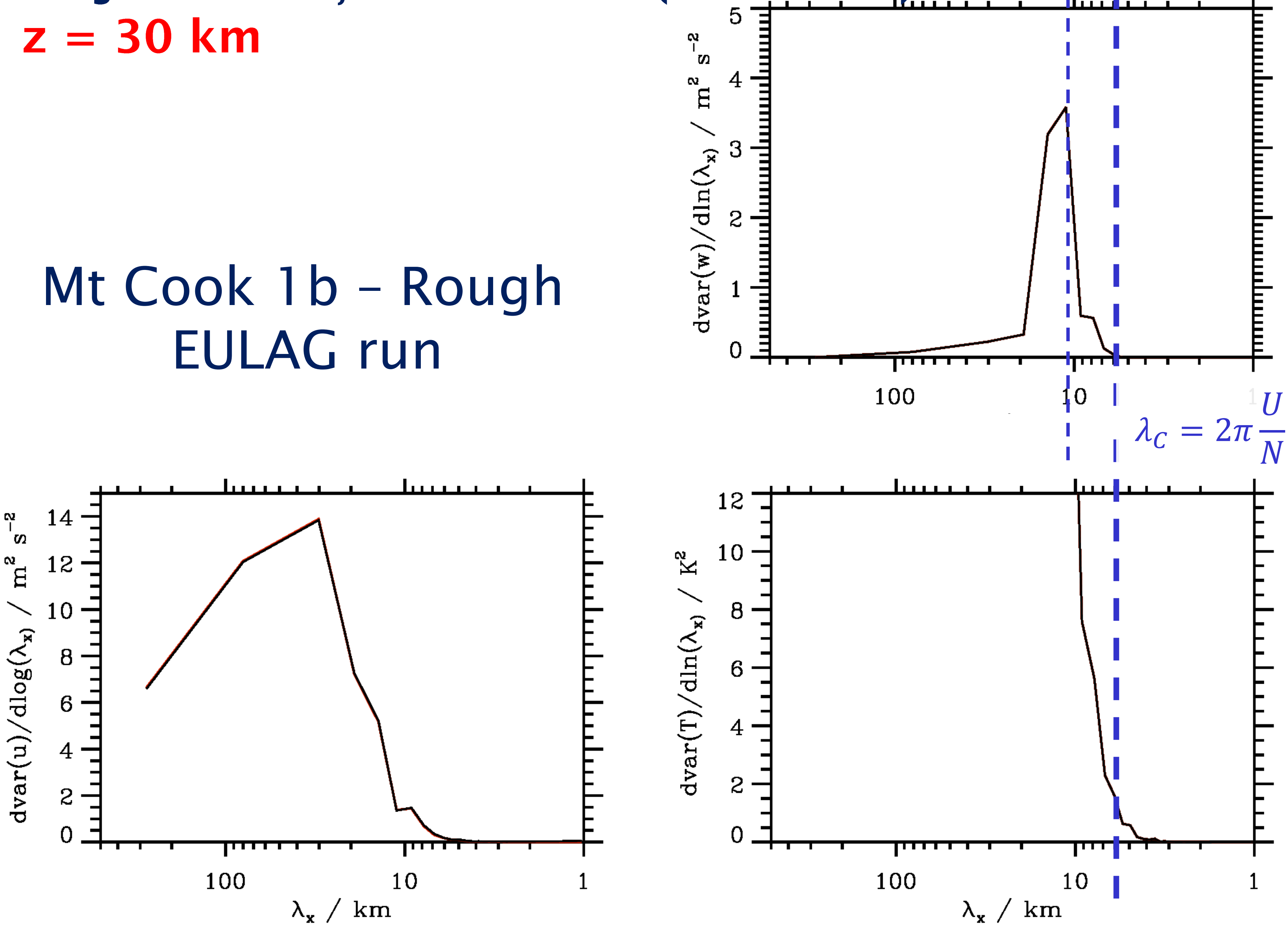

What about the roughness of NZ‘s terrain?

Mt Cook 1b

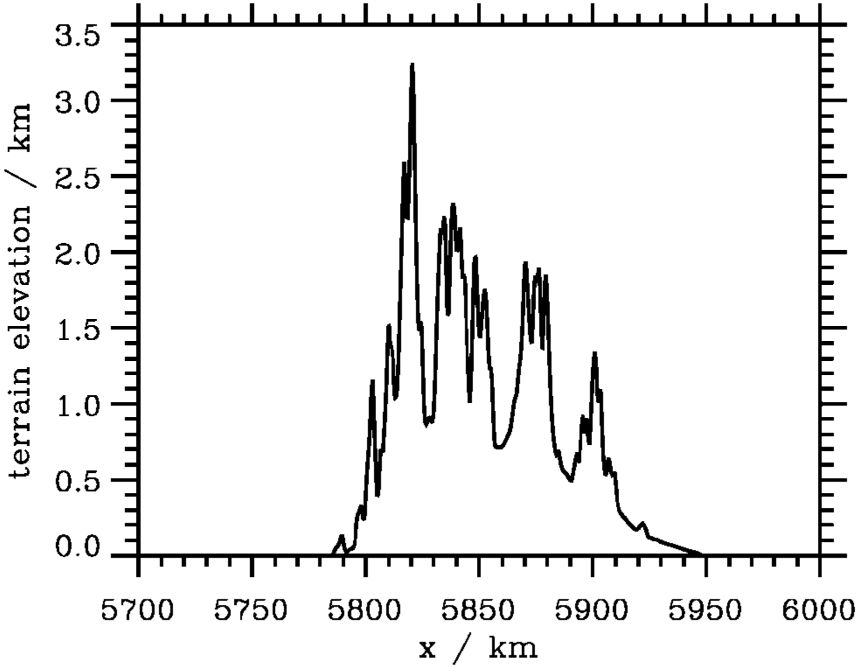
terrain elevation / km
3.5
3.0
2.5
2.0
1.5
1.0
0.5
0.0
5700
5750
5800
5850
5900
5950
6000
x / km

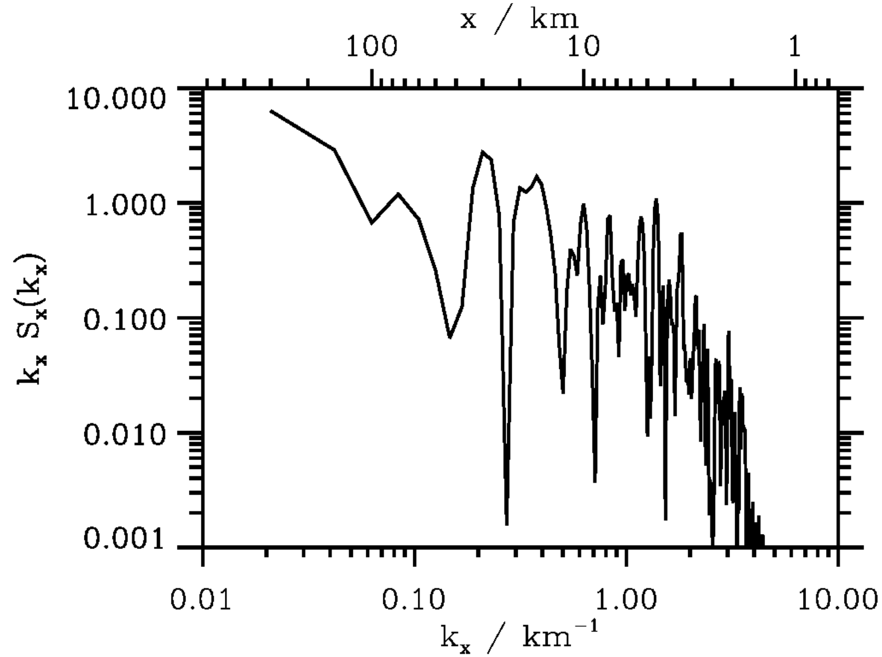
x / km
100
10
1
$k_x S_x(k_x)$
10.000
1.000
0.100
0.010
0.001
0.01
0.10
1.00
10.00
k_x / km^{-1}

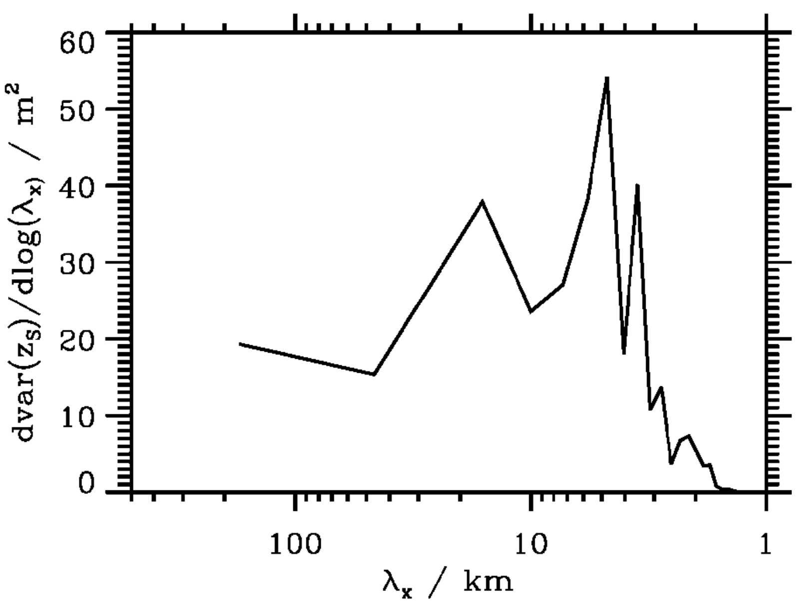
$dvar(z_S)/dlog(\lambda_x)$ / m^2
60
50
40
30
20
10
0
100
10
1
λ_x / km

Mt Cook 1b – Smoothed

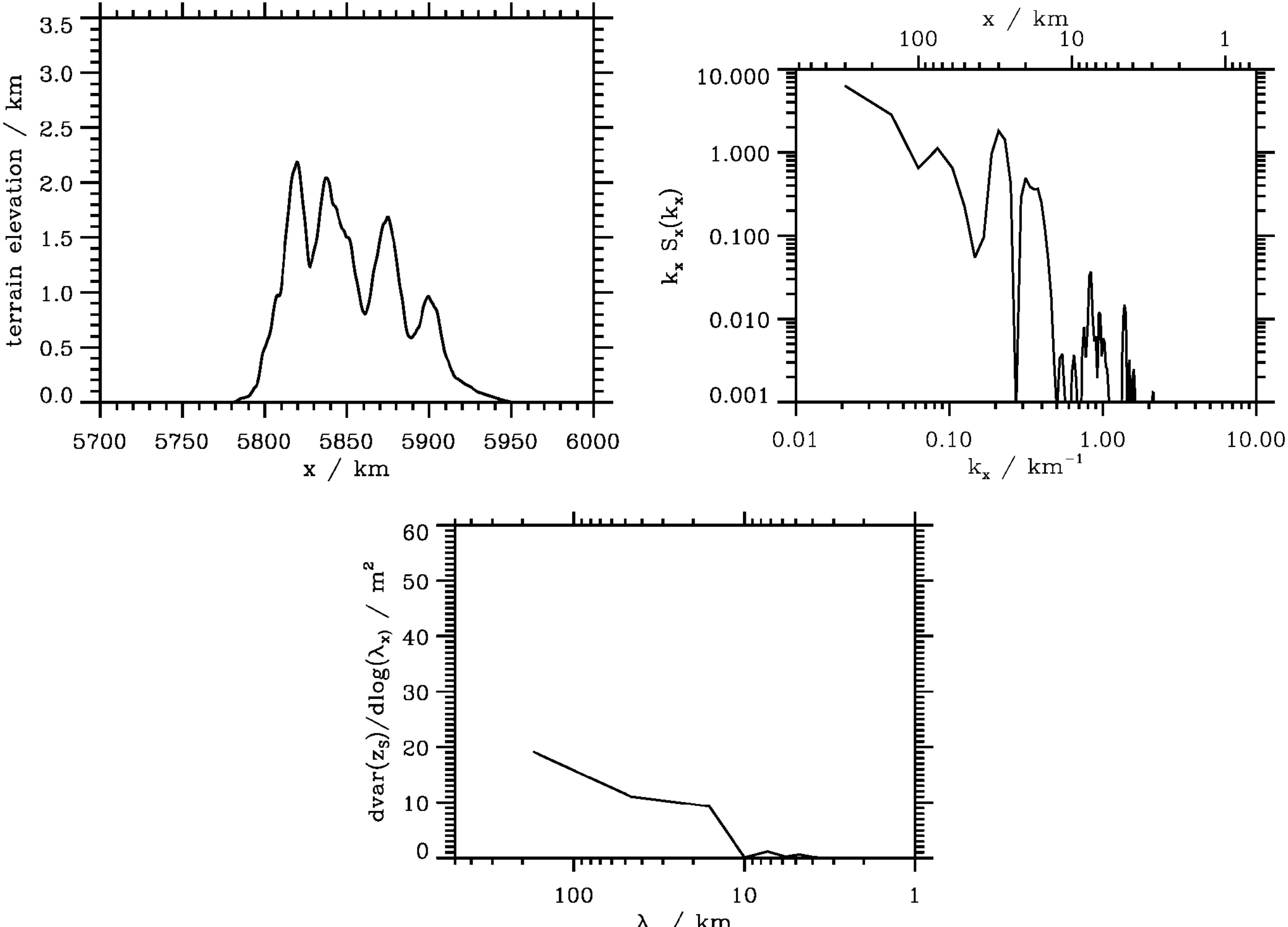

16 June 2016, Init: 12 UTC (+420 min)
z = 12 km

Mt Cook 1b – Smooth EULAG run

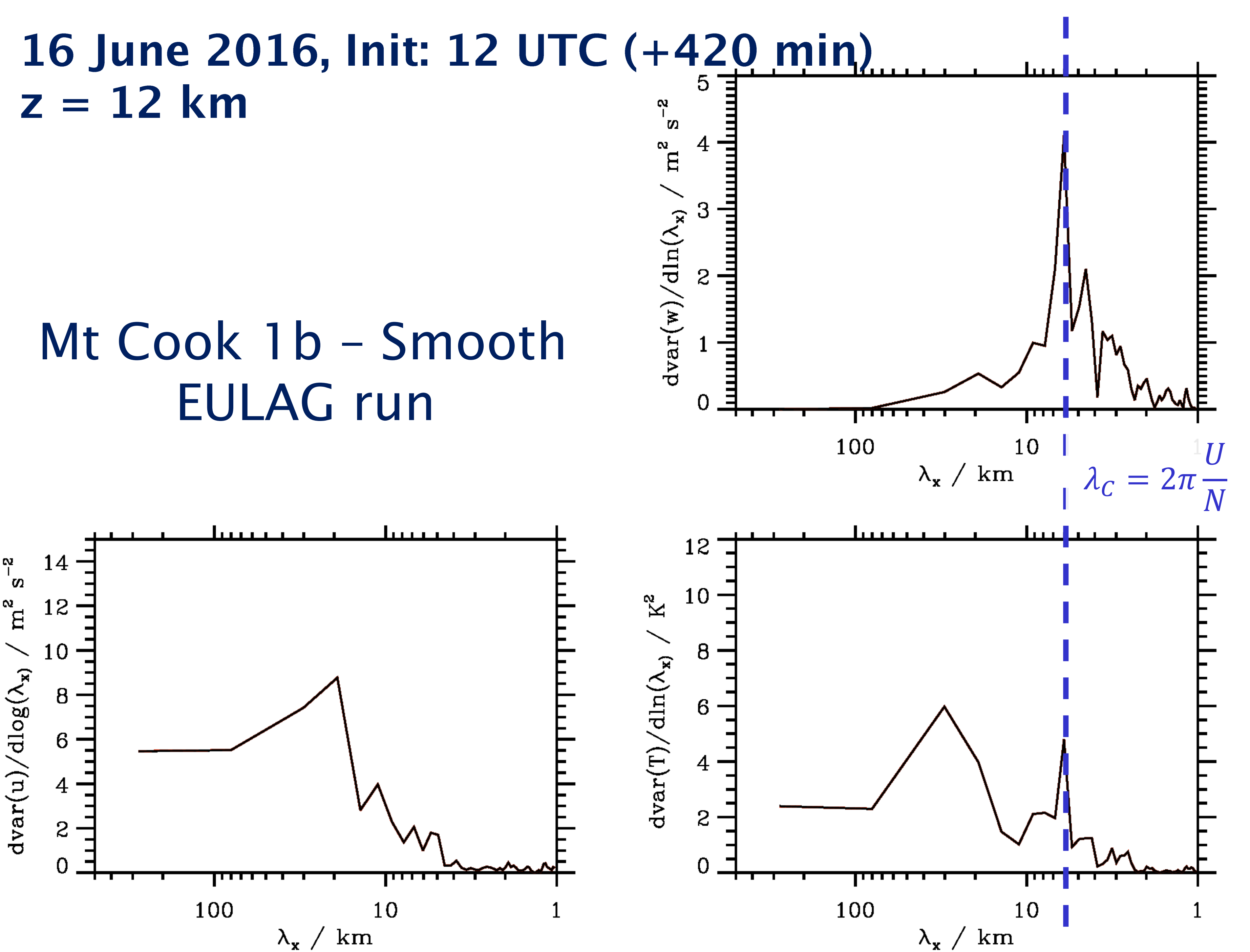

16 June 2016, Init: 12 UTC (+420 min)
z = 12 km

Mt Cook 1b – Rough EULAG run

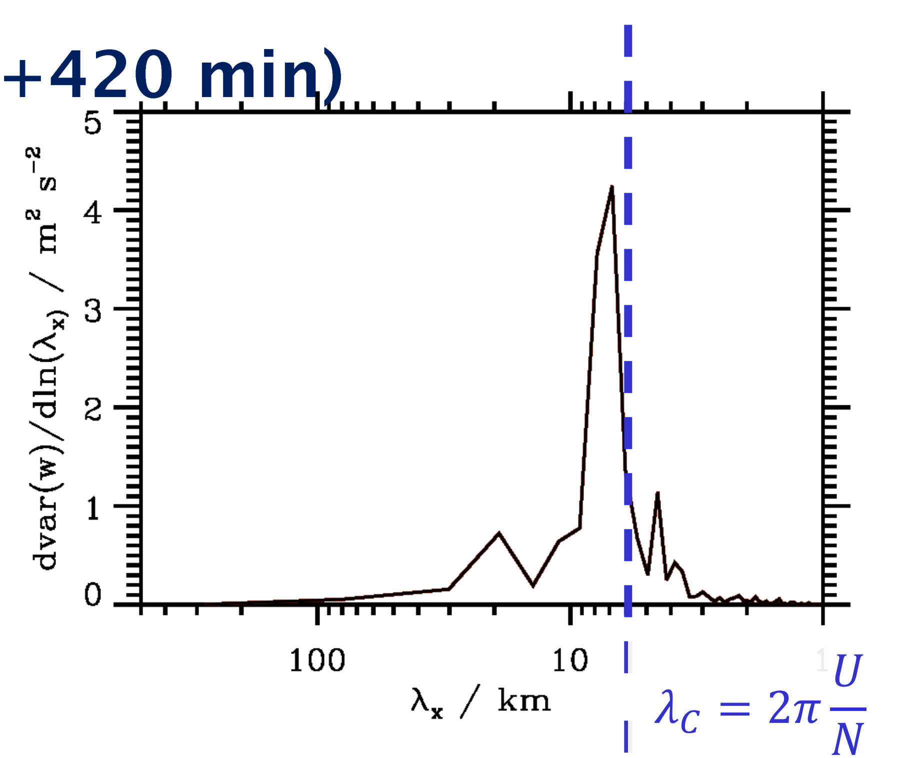

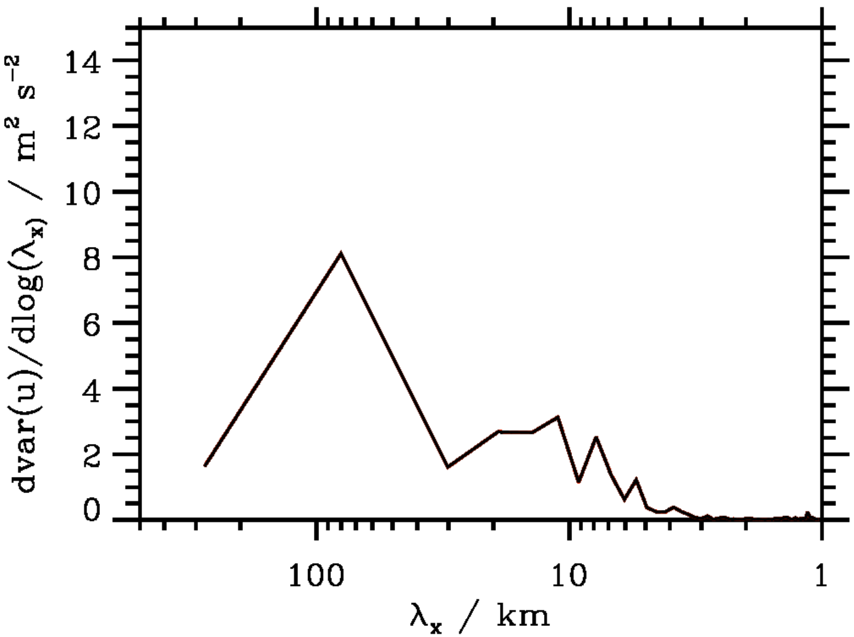

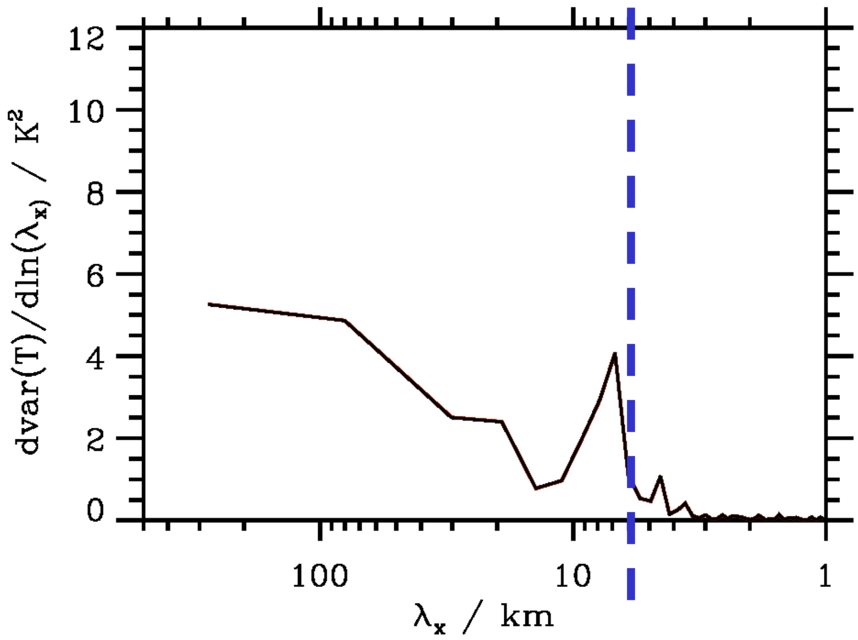

Dynamics in the upper troposphere and lower stratosphere

- EULAG simulations reproduce observed broad mountain wave spectrum with w-peaks at around 7 km (~ cut-off wavelength) and long-wavelength power in u and T

  → observed peaks in the w-spectrum are realizable in high-resolution numerical simulations

- roughness of the terrain does not seem to have an overwhelming impact on the spectra in the UTLS

  → wind filtering dominates the wavelength selection

AND/OR

→ wave trapping and interference with waves propating up- and downwards through the UTLS are the essential ingredients producing the observed spectra